AD-A077 555 NAVAL ACADEMY ANNAPOLIS MD F/G 20/6
THE KINETICS OF ION MOTION IN CAF2 :ER.(U)
JUN 79 D A BEAM
UNCLASSIFIED USNA-TSPR-97 NL

| OF |
ADA
077 555

END
DATE
FILMED
1 -80
DDC

LEVEL II

A TRIDENT SCHOLAR PROJECT REPORT

NO. 97

"THE KINETICS OF ION MOTION IN CaF2 :Er"

UNITED STATES NAVAL ACADEMY
ANNAPOLIS, MARYLAND

1979

(14) USNA-TSPR-97

27

U.S.N.A. - Trident Scholar project report; no. 97 (1979)

(6) THE KINETICS OF ION MOTION IN CaF_2:Er.

A TRIDENT SCHOLAR REPORT

BY

(10) MIDSHIPMAN DAVID ALAN BEAM CLASS OF 1979

U.S. NAVAL ACADEMY

ANNAPOLIS, MARYLAND

(9) Final rept. 1978-1979,

Donald J. Treacy

ADVISOR: ASSOC. PROF. DONALD J. TREACY

PHYSICS DEPARTMENT

(11) 8 Jun 79

ACCEPTED FOR TRIDENT SCHOLAR COMMITTEE

CM Reeter (12) 66

CHAIRMAN

8 June 1979

DATE

245600 DM

ABSTRACT

In this project, optical density versus wavelength was measured for $CaF_2:Er^{3+}$ crystals as a function of the temperature to which the crystals were heated prior to quenching. The quenching of the crystals had the effect of "freezing in" the high temperature equilibrium defect configurations in the crystal.

The results obtained support assignments of the optical absorption lines to various defect configurations. It was observed that the absorption line at 537.43 nm increased in height by a factor of about 20 as a result of heating and quenching, supporting the assumption that it is the result of a monomer defect site. The behavior of the absorption lines at 537.06 nm and 537.92 nm support the models that these lines are due to low order clusters.

The equilibrium among the defects of the $CaF_2:Er$ crystals can be described by an Arrhenius process characterized by an activation energy of 1.26 ± 0.02 eV.

The equilibrium, characteristic of the temperature from which the crystal was quenched, has

been modeled to be established by mobile interstitial fluorines.

TABLE OF CONTENTS

INTRODUCTION

Extensive studies have been conducted using calcium fluoride crystals doped with erbium, $CaF_2:Er^{3+}$. Each study has given fragmented bits of information answering many questions concerning the structure of the CaF_2:Er crystals and the erbium defect structures, but many questions have been left unanswered. This study was designed to investigate the equilibrium among various configurations of the point defects in the crystals, as a function of the temperature to which the crystals were heated prior to quenching.

As calcium fluoride models uranium oxide, used as fuel pellets and refractory materials in nuclear reactors, with the defects modeling the fission products in the fuel pellets, studying calcium fluoride doped with erbium may yield important information on how to more efficiently operate reactors.

In calcium fluoride, the calcium enters into the crystal lattice (a face centered cubic structure) as a divalent positive ion. The calcium fluoride structure may be viewed as a cubic array with a fluorine ion, F^-, at the corners of each cube and a calcium ion, Ca^{2+}, in the center of every other cube. When the CaF_2 crystals

are doped with erbium, some trivalent positive erbium ions, Er^{3+}, are substituted into the crystal lattice for calcium ions. The trivalent erbium ions cause a charge imbalance in the normal crystal structure. This electric charge is compensated for with the use of additional monovalent negative fluorine ions. (The additional fluorine ions come from erbium trifluoride which is the form in which the erbium is added to the melt from which the doped CaF_2 crystal is grown.) The negative fluorine ions charge compensate by locating themselves in various positions in the lattice, relative to the trivalent erbium ion.

Depending on the position of charge compensation, by the fluorine ions, different symmetries, relative to the erbium ion, can result. If the fluorine ion locally charge compensates an isolated erbium ion in a nearest neighbor interstitial position, a tetragonal site (C_{4v}) results yielding a fourfold rotational symmetry. If the fluorine ion locally charge compensates an isolated erbium ion along a body diagonal, a trigonal site (C_{3v}) results yielding a threefold symmetry. A fluorine ion non-locally charge compensating an isolated erbium ion, that is compensating at a relatively large distance away from the erbium ion, yields a cubic site with O_h symmetry.

It is possible that a cluster will form by erbium ions substituting for two or more neighboring calcium ions. When this occurs, the fluorine ions compensate the cluster. If two erbium ions replace neighboring calcium ions, a dimer site is formed. If three erbium ions replace neighboring calcium ions, a trimer site is formed, and so on.

In studying the CaF_2:Er crystals optically, the ^4f-->^4f transitions in the erbium ions were observed. The 4 of the ^4f transition corresponds to the principal quantum number of the transition. In the normal atom, the ^4f-->^4f transition is forbidden, which means that it has about 10^6 times less probability of occuring, than an allowed transition. This is because a ^4f-->^4f transition violates the selection rule which states that for an allowed transition, there must be a change in the orbital angular momentum quantum number of ± 1. (This selection rule specifies the condition, such that when a pair of wavefunctions describing the probable position of the electron, which violate this condition, are used in calculations with dipole matrix elements, the result of the calculations are zero.) The charge compensating fluorine ions create an electric field. This electric field causes perturbations in the wavefunctions of the electrons of the erbium ion. The

BACKGROUND

Alkaline-earth fluorides doped with rare-earth ions have undergone much investigation in recent years. In many of these investigations, the work has been done using crystals of alkaline-earth fluorides (MF_2) doped with trivalent positive rare-earth (RE) ions with the RE entering the crystal lattice substitutionally for some of the M ions. Methods of observation used in studying the crystals consist of such techniques as ionic thermo-currents (ITC), electron paramagnetic resonance (EPR), dielectric relaxation, optical spectroscopy, and ionic conductivity. Each of these techniques has yielded different information concerning structure, charge compensating mechanisms, defect site symmetries, energy levels for electron transitions, relative concentrations of defect symmetries, and changes in the crystals as a function of impurity concentration.

The first work relevant to this project was published by Weber and Bierig in 1964[1]. In their investigations they used both optical spectroscopy and electron paramagnetic resonance techniques. They postulated some of the initial ideas on charge

compensation mechanisms. Specifically, they observed changes in the EPR spectra as a function of crystal growth conditions (i.e. the effect of growing the crystal in an oxygen free atmosphere versus growth in an atmosphere containing oxygen which also enters the lattice substitutionally as O^{2-} ions, replacing F^- ions), and as a function of impurity concentration. In their results, they found that new lines appeared in both the optical and EPR spectra at high rare-earth concentrations, and suggested the existence of F^- ions in second nearest neighbor interstitial sites positioned along body diagonals yielding a trigonal symmetry and the possibility of the presence of pairs or clusters of ions.

One of the two papers of most significance used in this study was published in 1966 by Rector, Pandey, and Moos.[2] Using optical spectroscopy and EPR, they were able to give a definitive assignment of EPR lines to the different types of defect sites. By studying the Zeeman pattern as a function of rotational angle, Rector et al. also made a determination of the site symmetry of a number of spectral lines. In their study, they found that no lines were observed which were the result of defect sites with cubic symmetry, but they did find the existence of several trigonal

lines which were not as well defined as the predominant tetragonal lines.

Tallant and Wright did optical spectroscopy using laser selective excitation.[3] They observed fluorescent transitions of CaF_2:Er and classified the observations into sites having one erbium ion (monomer sites), and sites having more than one erbium ion (dimers, trimers, etc.). The sites with one erbium ion were determined to have tetragonal or trigonal symmetries. The defects with tetragonal symmetries were called A sites, while those with trigonal symmetries were called B sites by Tallant and Wright. The identification of the sites with more than one erbium ion, designated the C, D(1), and D(2) sites, was confirmed by ion-ion interactions. The defect sites with more than one erbium ion at the site had a strong dependence on dopant concentration. A tight energy coupling between the individual erbium ions was presumed to make up a given site. They found that one cluster site, the C site, had crystal field splittings similar to those of the B site, leading to the idea that the local environment sensed by the erbium ion is similar in both B and C sites. It was shown, however, that the C site could not be the result of a single Er-F pair, as is the B site, because there were more

transitions observed than could be explained as a result of the (2J+1)/2 levels of a single Kramer's ion. Dependence of the C, D(1), and D(2) sites on impurity concentration confirmed that these sites are the results of clusters since they disappeared for low concentrations. This confirmation was further strengthed by the observation of up-converted fluorescence in the C, D(1), and D(2) sites, and its absence in the A and B sites. The up-conversion is a result that can be observed only where multiple ion sites are present.

Fontanella and Andeen did important work in dielectric relaxation.[4] As concerned with this project, an important part of their work observed the effects of concentration dependence on dielectric relaxations. In their work they modeled the RII and RIV relaxations to be the result of clusters. The problem with their model, at that time, was that the RII cluster appeared in low concentration (0.001 mole-%) samples, contrary to the expected absence at such a low concentration. A qualitative quenching study was performed by Fenn, Wright and Fong, but their results were inconclusive.[5]

In very recent work, Fontanella, Treacy, and Andeen have done some correlative work between optical spectroscopy and dielectric relaxation.[6] Quenching CaF_2

:Er crystals from a temperature of 1120 K, they made quantitative comparisons between the "as received" and the after quenching results in optical spectroscopy and dielectric relaxation. They found that changes in the optical absorption peaks at 537.06 nm and 537.92 nm appeared to correlate with the RIV relaxation peak in dielectric relaxation. Of a possibly more significant note, they correlated the growth in the optical absorption band at 537.43 nm to the RII relaxation. The band at 537.43 nm corresponds to the trigonal defect site as reported by Rector et al.[2] This changes the idea that the RII relaxation peak is the result of clusters. They further correlated the RIII relaxation peak with the 538.88 nm and 539.52 nm peaks in the optical absorption spectra. In their work, they could not make a positive correlation between the RI peak and the optical absorption peaks except when crystals with low impurity concentrations were used. In the crystals with low impurity concentrations, the optical absorption peak at 539.40 nm, as reported by Rector et al., was able to be resolved.

EXPERIMENTAL PROCEDURE

For this investigation, $CaF_2:Er^{3+}$ 0.2 mole-% crystals were commercially obtained from Optovac Inc., as circular disks 25.4 mm in diameter. The preparation of the crystals began with the edges of the crystals being chamfered. The crystals were chamfered to prevent breakage in the next step of their preparation, that of being ground to the desired thickness of 1.5 mm. The crystals were ground using 14.5 micron aluminium oxide powder mixed with polishing oil (extender for polishing abrasives), both produced by Buehler, LTD. The edges of the crystals were again lightly chamfered and then the crystals were polished. For polishing, Metadi Diamond Polishing Compound (1 micron) and Metadi Fluid (extender for diamond paste) were used. After the crystals were polished, they were cleaned with acetone to remove any oils from their surfaces due to polishing and handling. The crystals were then cleaned with methanol to remove the acetone film left from their being cleaned with acetone.

A crystal was then selected to be placed in a dewar for initial measurements of the optical density versus wavelength (in nanometers) for the crystal in

the "as received" condition. The "as received" condition is that condition in which the crystal was received prior to any heating and quenching sequences. The crystal was held in the dewar by copper retainers. Silicone vacuum grease was applied to the copper retainers, and thereby to the crystal, to enhance thermal conductivity. The vacuum grease has a high thermal conductivity at low temperatures.

After the proper placement of the crystal in the dewar, the dewar was evacuated for a period of about 10-15 minutes to a pressure of about 30 microns. The dewar was then pre-cooled, to about 77 K, using liquid nitrogen. Once the dewar was pre-cooled, the liquid nitrogen was removed and the dewar was subsequently filled with liquid helium. When the dewar was filled with liquid helium, the thermal conductivity of the copper retainers and the silicone vacuum grease caused the temperature of the crystal to be about 10 K.

The crystal was cooled to reduce the random thermal motion in the crystal.

A reduction in the random thermal motion in the crystal was necessary to reduce the number of phonons within the crystal. A decreased number of phonons within the crystal caused a lower probability of disturbance of the transitions, giving the electron

transitions a longer lifetime.

With the crystal temperature being held constant, by the liquid helium, at about 10 K, the dewar was positioned in the Cary 17 dual beam recording spectrophotometer for initial measurements of the optical density versus wavelength (in nanometers) for the crystal in the "as received" condition. Initial measurements were made over the range of 180 to 550 nanometers, to locate the optical absorption bands. Measurements were again taken for the bands between 435 and 545 nanometers, 360 to 380 nanometers, and 250 to 265 nanometers. The crystal was then removed from the dewar and was cleaned with acetone and methanol in preparation for the heating and quenching processes.

Prior to the heating process, a thermal profile was made of the furnace yielding temperature versus position data on the Diffusitron Furnace. The thermal profile was made using iron-constantan and chromel-alumel thermocouples. A typical profile measured on the furnace used in this project appears in figure 7. The thermocouples were constructed using a glass inner-tube containing one wire, and a quartz outer-tube containing the inner tube with its wire, and an additional wire. The thermocouples were calibrated using an ice bath and a boiling water bath. After cleaning, the crystal was

put on a holder, called a boat due to it being shaped similarly to a canoe, and inserted into a quartz vacuum tube

The vacuum tube had been previously cleaned by washing with a NaOH solution, rinsing with water, and drying by heating in the furnace for several hours. Due to the dynamic vacuum applied to the quartz tube throughout the drying period, the period also had the effect of baking out any impurities which could have possibly contaminated the crystals during subsequent heating and quenching processes.

The quartz tube containing the CaF_2:Er crystal was then evacuated. A roughing pump was used to evacuate the tube to a pressure of 100 microns, and then a diffusion pump was used in conjunction with the roughing pump to reduce the pressure within the quartz tube to 2×10^{-6} Torr. In addition to the two dynamic pumps, the system was cold trapped using the liquid nitrogen which had been poured off earlier from the dewar pre-cooling stage in this procedure. The cold trapping had the effect of freezing out any atmosphere remaining after the use of the dynamic pumps, thereby further increasing the vacuum within the quartz tube and stopping back flow from the diffusion pump. The crystal was heated under a vacuum to prevent possible

oxygen contamination. Oxygen contamination results from oxygen, in the form of O^{2-}, substituting into the crystal lattice for fluorine ions. Oxygen contaminated crystals yield different optical absorption spectra than the uncontaminated crystals.

After reducing the pressure within the quartz tube, the crystal was ready to be heated. The furnace was set at the desired temperature and allowed to reach an equilibrium. The temperature of the furnace was checked, using the thermocouple, and was held to an accuracy of $\pm$ one kelvin. The quartz tube, containing the crystal under the dynamic vacuum, was then inserted into the furnace. The crystal was the heated for a two hour period. After the two hour heating period, the quartz tube, containing the crystal, was removed from the furnace. The crystal was then allowed to cool radiatively at an initial rate of about 50 K per second. After the cooling period, the pressure in the quartz tube was increased to atmospheric pressure. The crystal was then removed from the quartz tube and lightly polished to remove any vacuum oil from the surface. After polishing, the crystal was again cleaned with acetone and methanol. The crystal was then reinserted into the dewar in preparation for more optical absorption measurements using the Cary 17.

RESULTS

The E manifold of the CaF_2:Er crystals was studied extensively. The range of wavelength for the E manifold is from 534 nm to 541 nm. Measurements of the optical density versus wavelength were obtained for various temperatures from which the crystal had been quenched. Measurements were taken on the crystal in the "as received" condition, and after the crystal had been quenched from temperatures of 723 K, 783 K, and at 25 K intervals over the temperature range of 873-1048 K, inclusive. The results of the measurements are displayed in figures 2 - 13. Although the data was taken as continuous spectra, it is displayed in this report as series of points as the result of being digitized.

DISCUSSION OF RESULTS

Plots of the optical density versus wavelength, of the E manifold, for CaF_2:Er crystals in the "as received" condition are shown in figures 2 and 3. Appearing in each plot, of figures 2 and 3, are two relatively strong absorption lines, two relatively weaker absorption lines, and one barely resolvable absorption line. The two relatively strong absorption lines have their peaks at 538.88 nm and 539.52 nm. The two relatively weaker absorption lines peak at 537.06 nm and 537.92 nm. The barely resolvable absorption line has its peak at 537.43 nm. The heights of the absorption lines, measured in units of optical density, are directly proportional to the concentrations of the defect sites, within the crystals, causing the absorptions. The proportionality implies that the greater the optical density, at a particular wavelength, the greater number of defect sites present which give rise to the absorption at that wavelength.

The normal process for determining changes in the optical density of the crystals is one based on the product of the absorption linewidth and the absorption line height. To determine these values, APL programs

were developed for curve fitting by Captain P. J. Kimble, USMC, and appear in the appendix. In this project, it was observed that using the product of height times linewidth as a function of the temperature from which the crystals were quenched yielded the same information as if just the absorption height were used as a function of the temperature from which the crystals were quenched. Although extensive curve fitting for the absorption lines of the E manifold was conducted in this project, the activation energies determined were based on calculations using the absorption line heights as a function of the temperature from which the crystal was quenched.

Absorption lines at 538.88 nm and 539.52 nm:

The optical density of the absorption lines at 538.88 nm and 539.52 nm appear to decrease monotonically as the temperature from which the CaF_2:Er crystals were quenched increases. These absorption lines may be identified as the D sites of Tallant and Wright and the RIII relaxation peak in dielectric relaxation. The change in optical density as a function

of the temperature from which the crystals were quenched can be described as Arrhenius processes with activation energies of -1.25 ± 0.04 eV and -1.26 ± 0.15 ev, respectively for the absorption lines at 538.88nm and 539.52 nm. The decrease in the optical density begins at about 948 K and essentially goes to completion when the temperature from which the crystals were quenched reaches 1048 K. The decrease in the optical density, as the temperature from which the crystals were quenched increases, is consistent with the erbium cluster models proposed to describe the RIII relaxation peak and the D sites of Tallant and Wright. The cluster models describe the RIII relaxation peak and the D sites to be the result of erbium ion clusters of a higher order than dimer.

It is interesting to note that after thermally removing the absorption line peaking at 539.52 nm, the residue peaking at 539.40 nm corresponds to the absorption line resulting from defect sites having tetragonal symmetries, as reported by Rector et al., and the A site of Tallant and Wright. From the work of Fontanella, et al, a positive relation between the absorption line at 539.40 nm and the RI relaxation peak was not defined except in crystals of low impurity concentrations, where the absorption line at 539.52 nm

was not present.

It is also important to note that the decreases in the absorption lines at 538.88 nm and 539.52 nm appear to saturate when the crystals were quenched from temperatures greater than 1048 K. This is observed by adding the 1173 K data point reported in work by Fontanella, Treacy and Andeen.[6] The addition of this data point is valid in the sense that the crystals used in their investigation were grown from the same melt as those used in this investigation, and that their "as received" spectra of the E manifold were the same as those observed in this investigation.

Absorption line at 537.43 nm:

The optical density of the absorption line at 537.43 nm appears to increase monotonically as the temperature from which the CaF_2:Er crystals were quenched increases. This absorption line may be identified as the B site of Tallant and Wright, the defect of trigonal symmetry, as reported by Rector et al., and the RII relaxation peak of dielectric relaxation. The change in the optical density as a

function of the temperature from which the crystals were quenched can be characterized as an Arrhenius process with an activation energy of 1.30 ± 0.12 eV. The increase in optical density begins at 948 K, the temperature from which the crystals were quenched at which cluster break up began. Again, it is seen that this process is essentially complete at 1048 K, after increasing its optical density by a factor of about 20 over the crystal in the "as received" condition. The behavior of this absorption band is consistent with what would be expected for a monomer, a defect site with only one erbium ion present. As seen in figure 16, the natural logarithm of the optical density, starting at about -6, implies that prior to quenching the crystals from temperatures higher than 873 K, there were few trigonal sites present. Consequently, this may resolve some of the conflicts in the literature over the existence or non-existence of a trigonal defect in calcium fluoride crystals doped with trivalent rare earths of a smaller ionic radius than gadolinium. Whether a trigonal will or will not be observed is a function of the crystal thermal history.

It is also most interesting to note the appearance of an absorption line at 537.89 nm, as the temperature from which the crystal was quenched became

greater than 948 K. This absorption line corresponds to the second position of a B site fluorescence line noted by Tallant and Wright. As this line was not able to be resolved when the crystals were quenched from low temperatures, a positive correlation between it and the absorption line at 537.43 nm has not been made in this project.

Absorption lines at 537.06 nm and 537.92 nm:

Probably the most interesting results of this investigation are the changes in the optical density as a function of the temperature from which the CaF_2:Er crystals were quenched for the absorption lines at 537.06 nm and 537.92 nm. It is seen that as the temperature from which the crystals were quenched increases, there is first a decrease and then an increase in the optical density at 537.06 nm and 537.92 nm as seen in figure 17.

These absorption lines have been identified with the RIV relaxation peak and with the C site of Tallant and Wright. The observation that the ratio of the relative heights of these absorption lines is a

constant equal to 1.86 ± 0.08 supports the conclusion that these lines have the same defect site origin.

If this absorption line actually is the result of a dimer defect site,as reported in the literature, then the initial decrease in optical density, as the temperature from which the crystals were quenched increased, is consistent with the break up of clusters. This initial decrease can be characterized by an Arrhenius process with an activation energy of 0.44± 0.01 eV. It also has been observed that while this cluster break up is occurring, there is a slight increase in the optical density of the absorption lines due to monomer defect sites.

It is further consistent that as the lowest order cluster allowable, that as the higher order clusters break up, they might cause an increase in the concentration of not only the monomer defect sites, but also the lowest order cluster (dimer) defect sites. The concentration of the dimer defect sites would increase only if the higher order clusters breaking up were capable of feeding the dimer defect sites faster than the dimers wished to break up.

In this investigation, it was found that the increase in the optical density for the absorption lines associated to the dimer defect sites began at

about the temperature where the higher order clusters began to break up. The increase in the dimer site concentration, as a result of the break up of the higher order clusters, can be characterized by an Arrhenius process with an activation energy of 1.25 ± 0.07 eV.

The activation energy of 1.26 ± 0.02 eV characterizing the Arrhenius process which describes the equilibrium among the defects of the crystals was determined using a weighted average. The weight given to each value of activation energy was inversely proportional to the uncertainty of the particular value of activation energy.

An Arrhenius process is one that can be described by an exponential function. In this investigation, changes in the optical density as a function of the temperature from which the crystals were quenched can be characterized by an Arrhenius process with the defining equation for the Arrhenius process being

$$N=N_o \exp(-E/kT).$$

In this equation, N corresponds to the number of defects in a specific configuration presently in the

crystal. N_o corresponds to the number of defects present in a specific configuration at some reference point in the history of the crystal, E corresponds to the activation energy for the Arrhenius process, k refers to Boltzmann's constant, and T refers to the temperature from which the crystal was quenched. In this project, relative values for N and N_o were used, based on the heights of the absorption lines which were directly proportional to N and N_o.

CONCLUSIONS

Considering all the literature available, the changes observed in the optical absorption spectra as a function of the temperature from which the crystals were quenched can be most consistently modeled to be the results of fluorine ion motion. This model holds when the activation energies characterizing the Arrhenius processes are considered. This model is further supported by the saturations of the changes in the optical absorption spectra as the temperatures from which the crystals were quenched increased beyond 775° C.

Subsequent investigations for this project should include a study of changes in the optical absorption spectra as a function of quenching the crystals from temperatures higher than 900 °C. It is possible that the equilibria attained at temperatures greater than 900 °C would be the result of motion of the trivalent erbium ion. Also in such a study, quenching may be done to rapidly cool the crystal to liquid nitrogen temperatures or cooler rather than to room temperature, as was done in this project. This would probably yield greater changes in the optical absorption spectra, as a

function of temperature from which the crystal was quenched, due to a reduction of the diffusion of untrapped fluorine ions through the crystal lattice. Theoretically, the untrapped fluorine ions can diffuse through the lattice, at room temperatures, thereby causing the quenching to not completely "freeze in" the high temperature defect equilibria.

Another possible study motivated by this project would be that of a correlation of the changes in the optical absorption spectra with those in dielectric relaxation, as a function of the temperatures from which the crystals would be quenched. Although not discussed in this project report, the increase in the optical density of the 483.25 nm absorption line in the G manifold appears to be related to the growth of the RI peak in dielectric relaxation. Both the increse in the optical density, and the growth in the RI peak appear to be characterized by an activation energy of about 0.7 eV.

ACKNOWLEDGEMENTS

I would first like to thank Professor Donald J. Treacy for the great patience, endurance and trust which he displayed throughout the year. I also really appreciate the many discussions we shared on topics other than physics, concerning life in general. I also would like to thank Captain R. J. Kimble for his time and effort in writing the curve fitting programs. I really appreciate the assistance of Professor Fontanella, especially his teaching me the 'ins and outs' of the computer. I desire to also thank Mr. Charles Stump for his outstanding technical support in keeping the Cary running. It would also be unfair if I did not mention all the loving support that I received from my mother, Dr. Lillian K. Beam, by way of her letters and long distance phone-calls from San Diego, California. I wish to express my gratitude to everybody else who helped me in any way in the completion of this project. My acknowledgements would not be complete without thanking God for the peace, strength, and the abilities which I received, through my Lord and Savior Jesus Christ, for the completion of this project.

REFERENCES

1. M. J. Weber and R. W. Bierig, Phys. Rev. 134, A1492 (1964).

2. C. W. Rector, B. C. Pandey, and H. W. Moos, J. Chem. Phys. 45, 171 (1966).

3. D. R. Tallant and J. C. Wright, J. Chem. Phys. 63, 2074 (1975).

4. C. Andeen, D. Link, and J. Fontanella, Phys. Rev. 16, 3762 (1977).

5. J. B. Fenn, Jr., J. C. Wright, and F. K. Fong, J. Chem. Phys. 59, 5591 (1973).

6. J. Fontanella, D. Treacy, and C. Andeen, to be published.

FIGURE 1

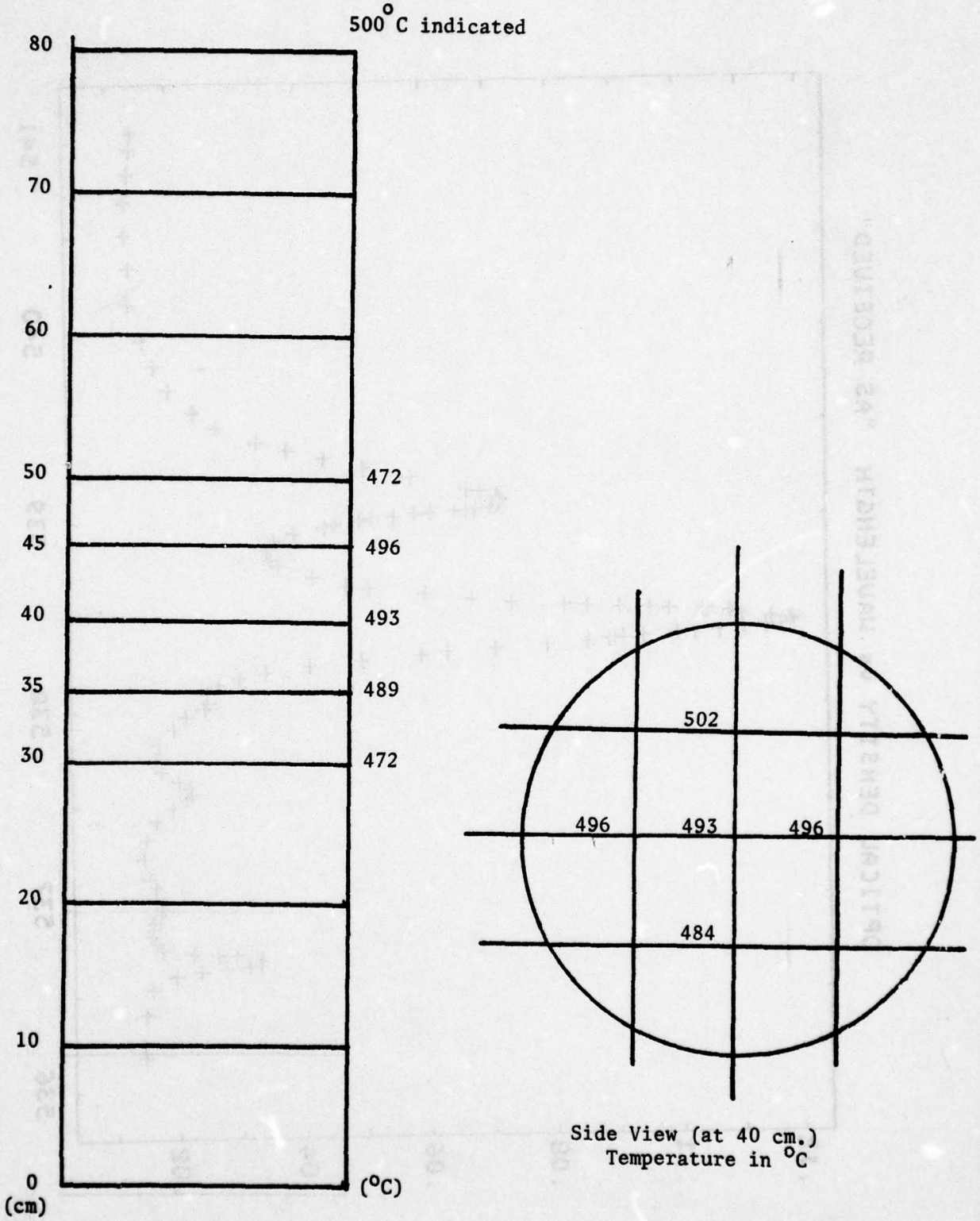
500 °C indicated
80
70
60
50
45
40
35
30
20
10
0
(cm)
472
496
493
489
472
(°C)
Top View
502
496
493
496
484
Side View (at 40 cm.)
Temperature in °C

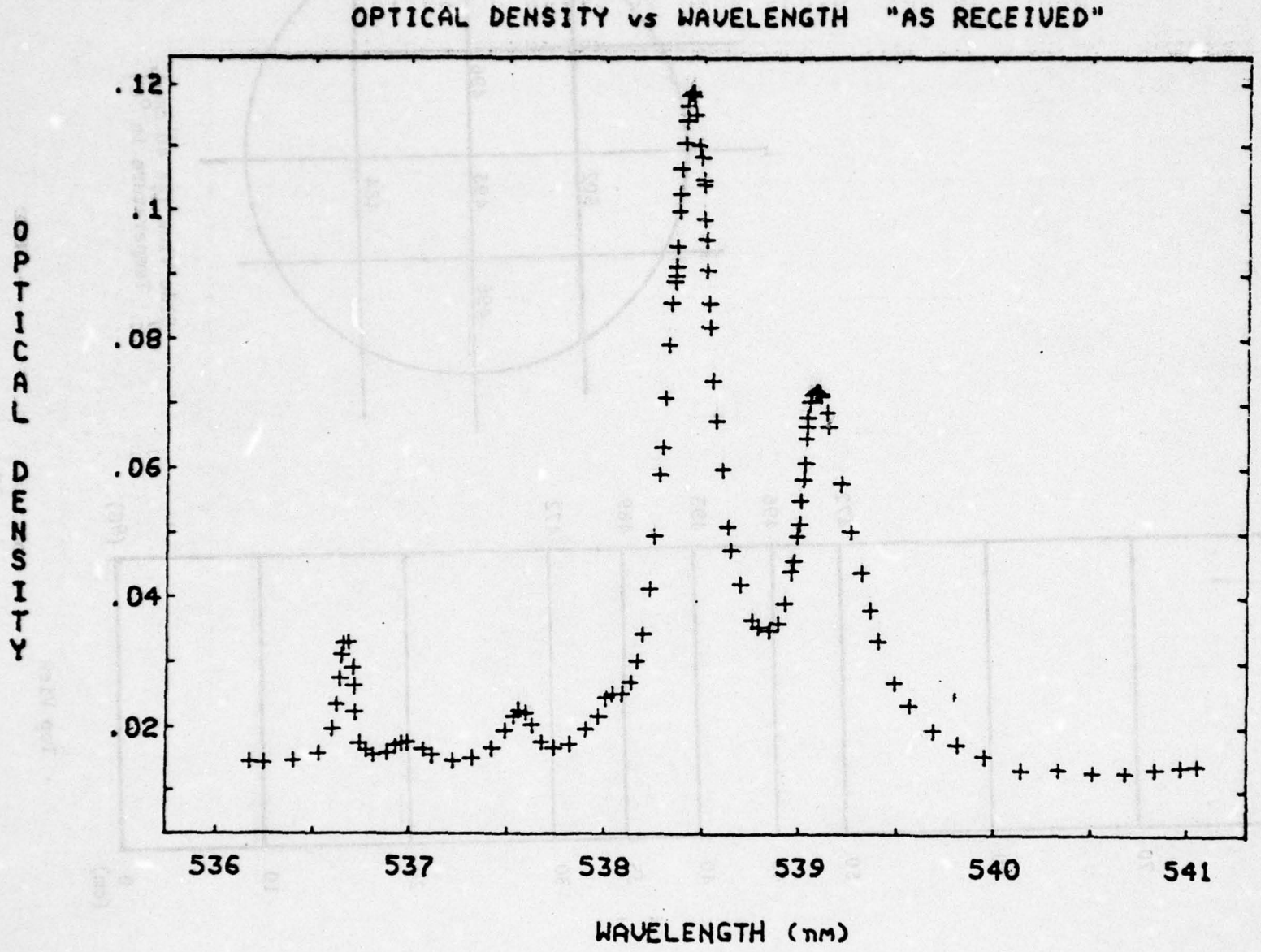
OPTICAL DENSITY vs WAVELENGTH "AS RECEIVED"
OPTICAL DENSITY
.12
.1
.08
.06
.04
.02
536
537
538
539
540
541
WAVELENGTH (nm)

FIGURE 2

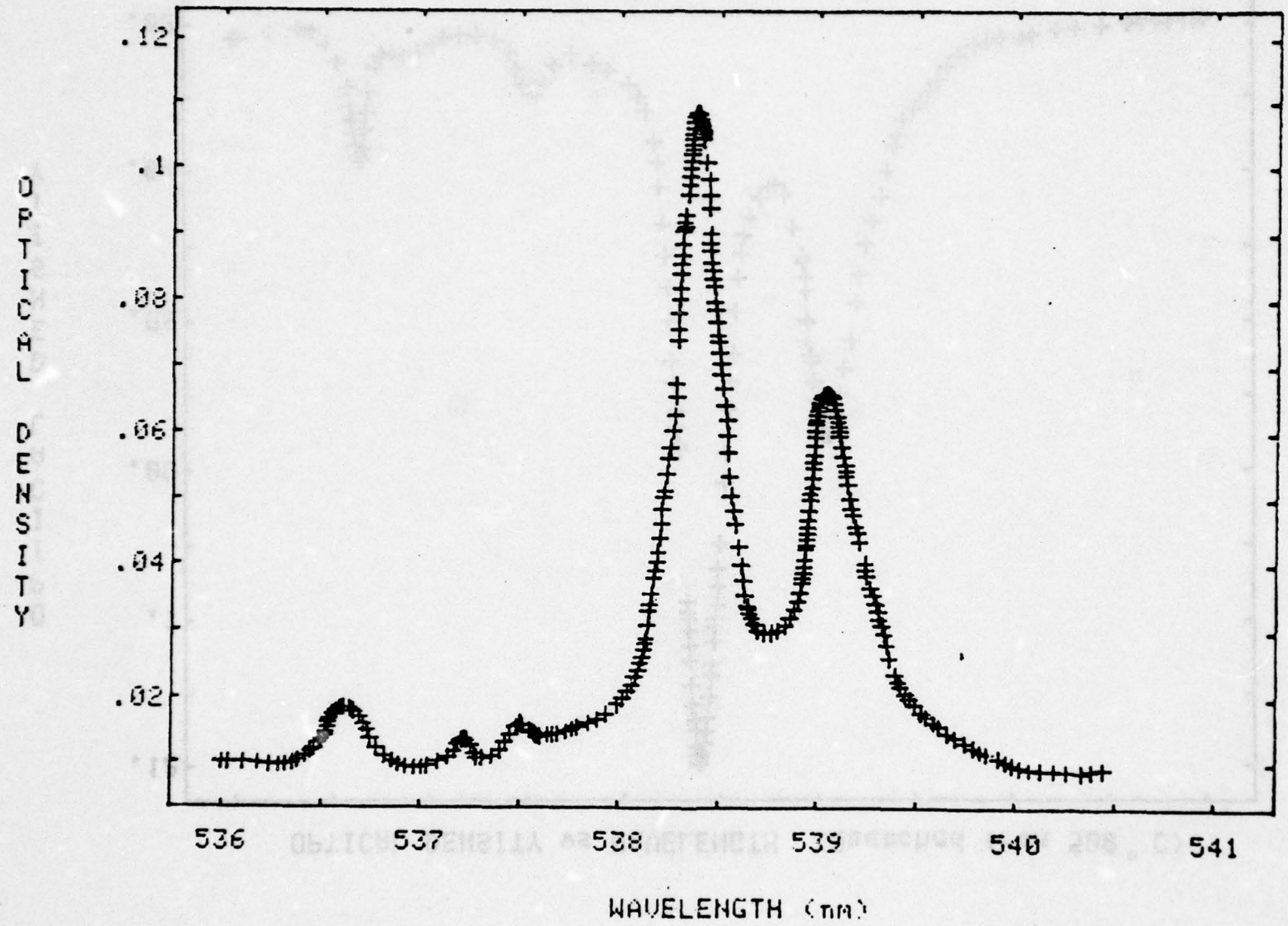
OPTICAL DENSITY vs WAVELENGTH "AS RECEIVED"
OPTICAL DENSITY
.12
.1
.08
.06
.04
.02
536
537
538
539
540
541
WAVELENGTH (nm)

FIGURE 3

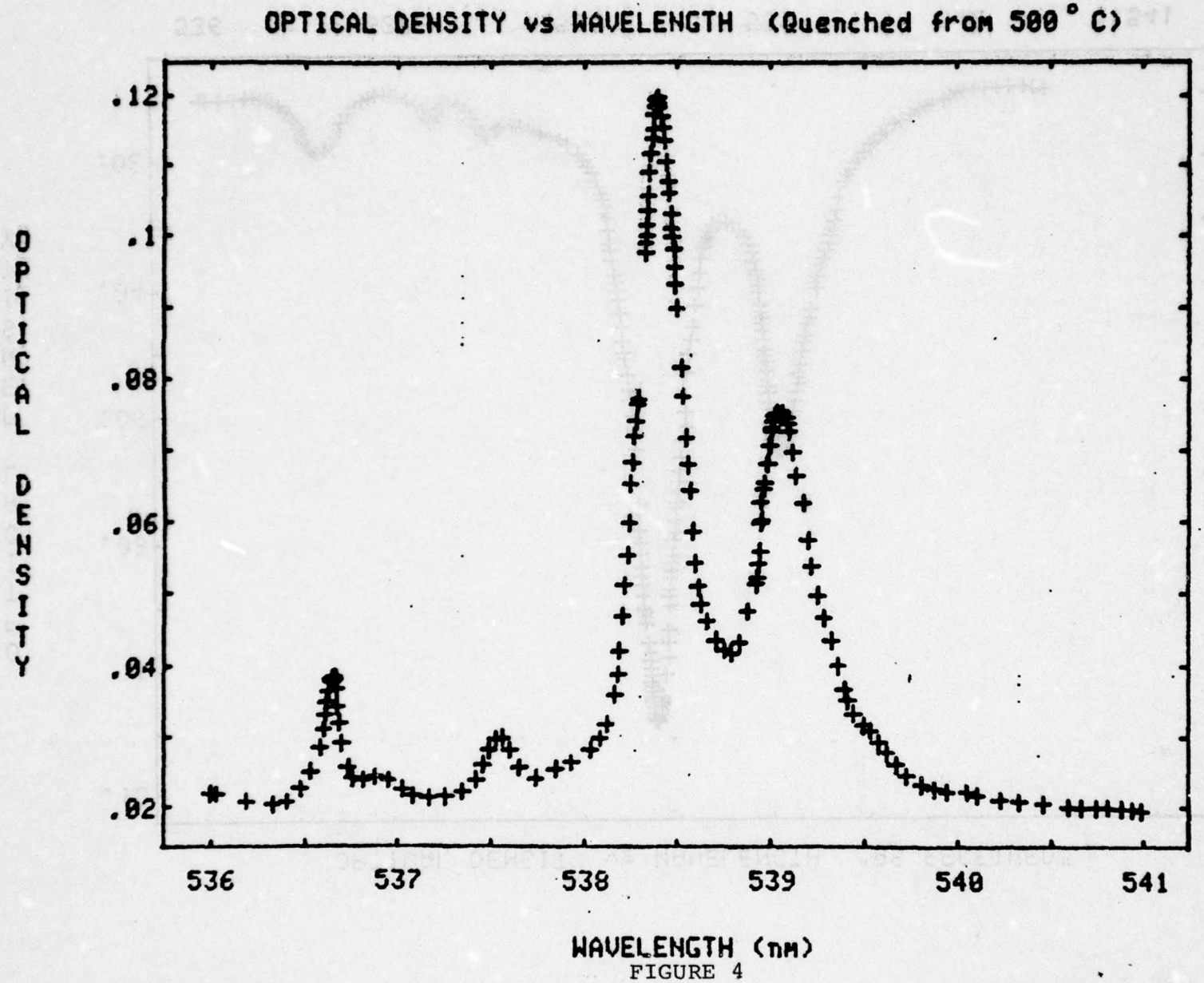
OPTICAL DENSITY vs WAVELENGTH (Quenched from 500° C)
OPTICAL DENSITY
.12
.1
.08
.06
.04
.02
536
537
538
539
540
541
WAVELENGTH (nm)

FIGURE 4

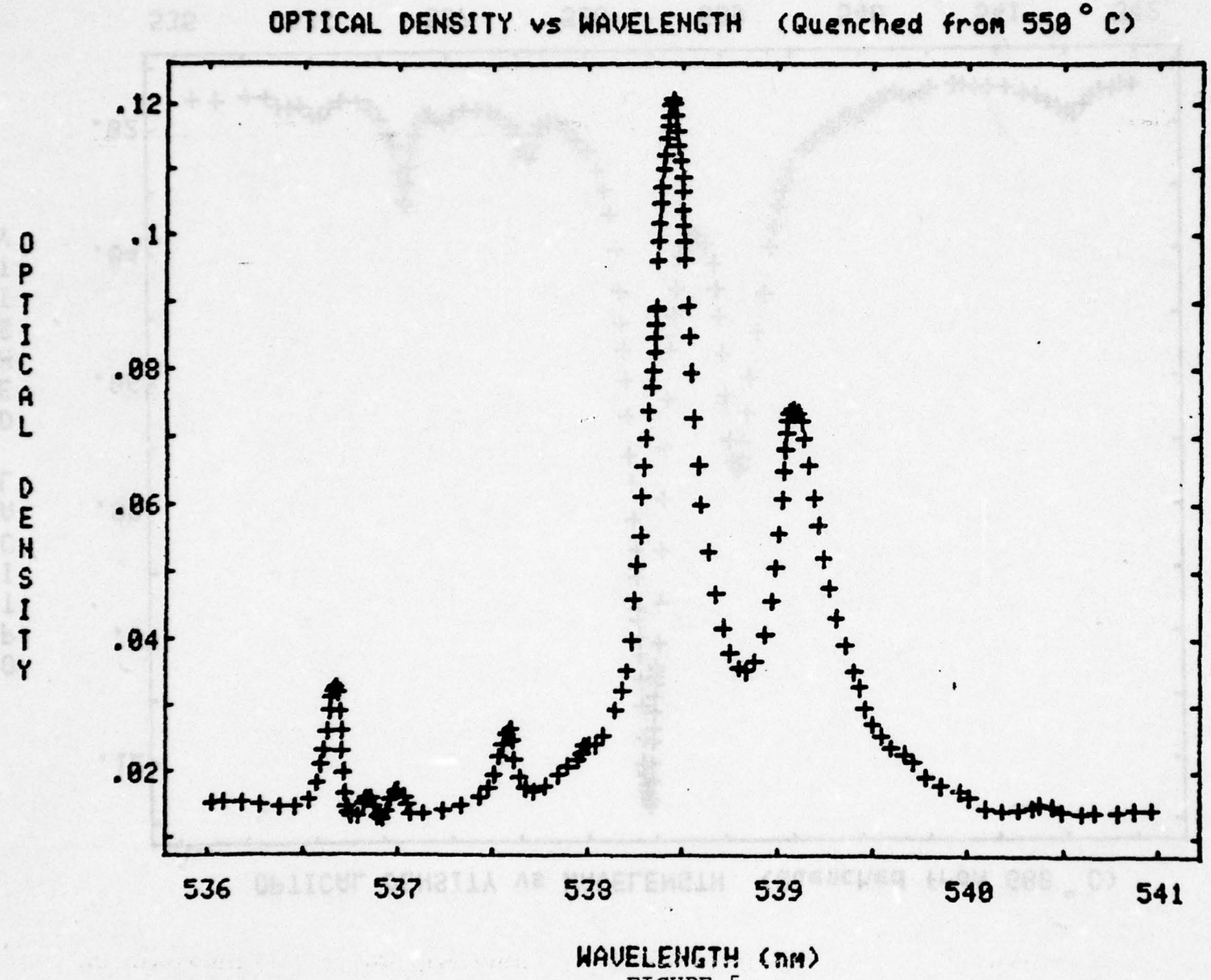
OPTICAL DENSITY vs WAVELENGTH (Quenched from 550 ° C)
OPTICAL DENSITY
.12
.1
.08
.06
.04
.02
536
537
538
539
540
541
WAVELENGTH (nm)

FIGURE 5

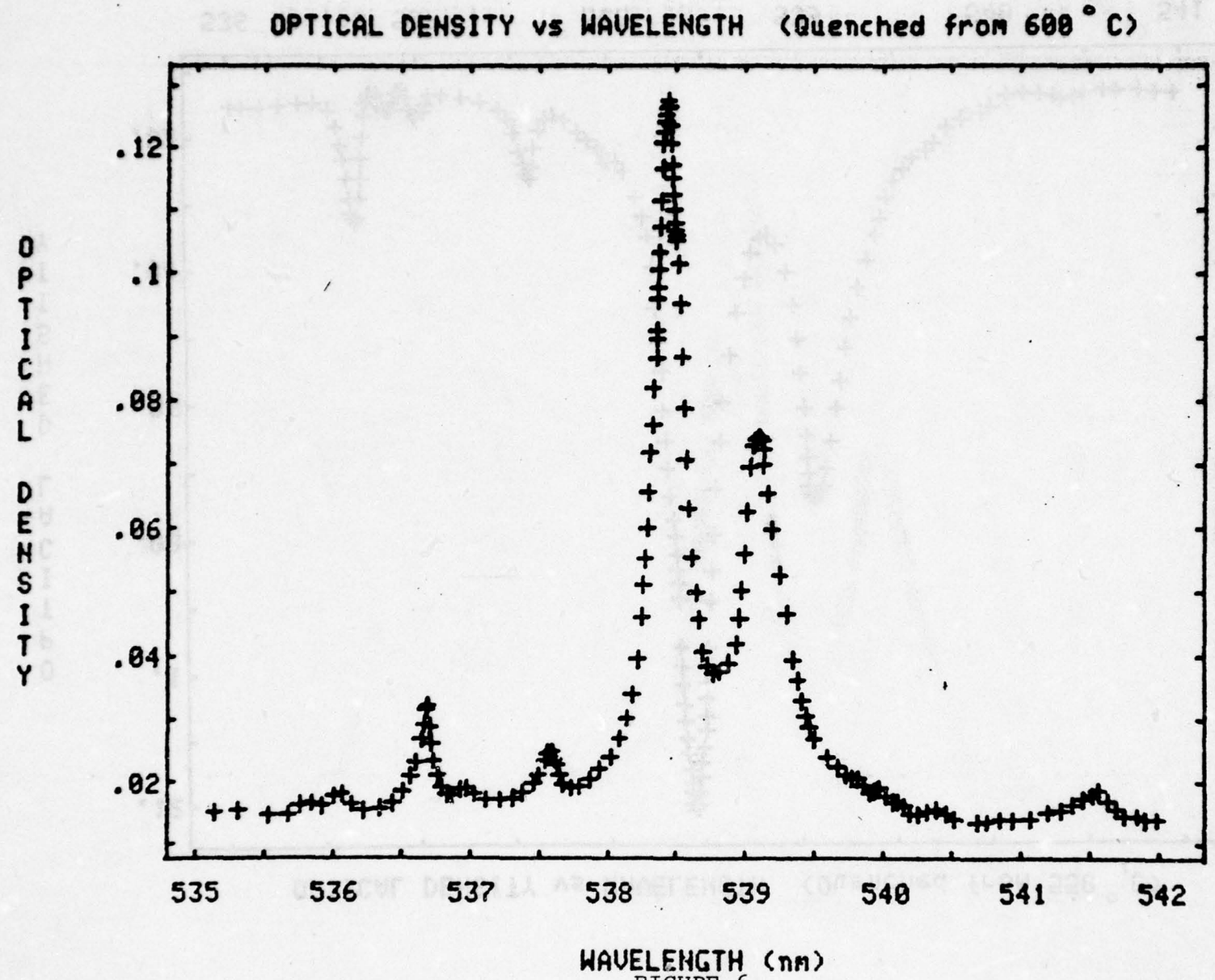
OPTICAL DENSITY vs WAVELENGTH (Quenched from 600 ° C)
OPTICAL DENSITY
.12
.1
.08
.06
.04
.02
535
536
537
538
539
540
541
542
WAVELENGTH (nm)

FIGURE 6

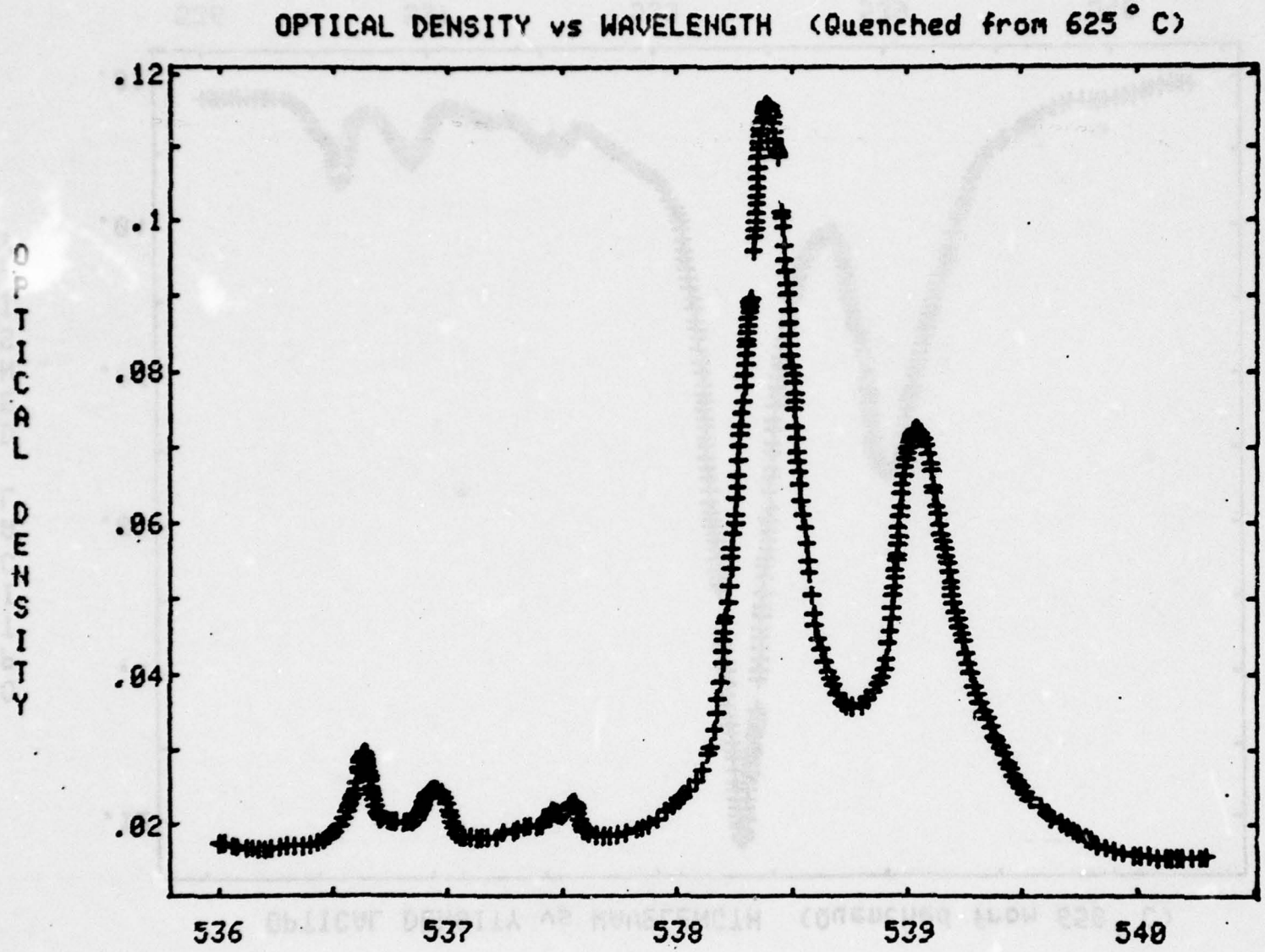
OPTICAL DENSITY vs WAVELENGTH (Quenched from 625° C)
.12
.1
.08
.06
.04
.02
OPTICAL DENSITY
536
537
538
539
540
WAVELENGTH (nm)

FIGURE 7

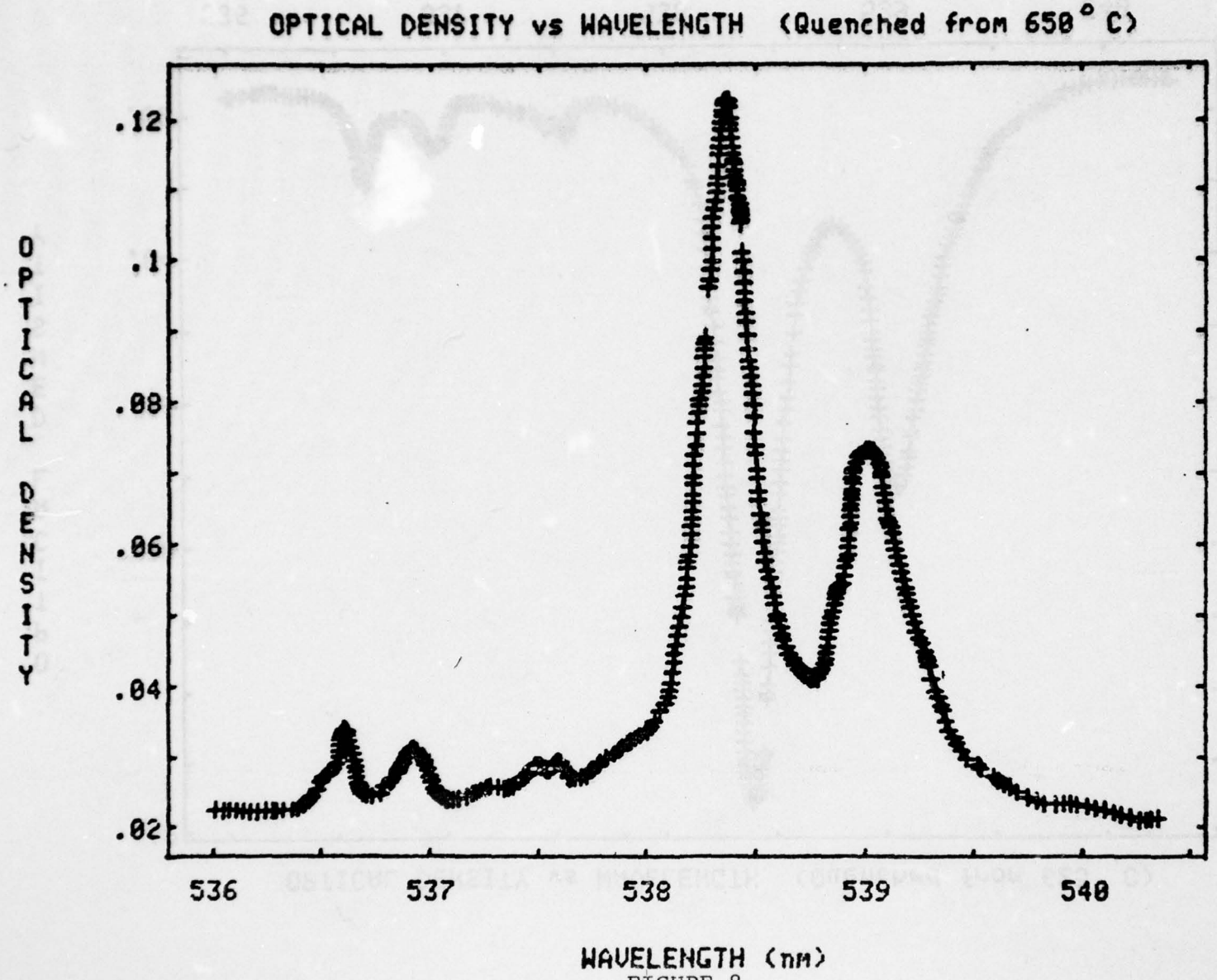
OPTICAL DENSITY vs WAVELENGTH (Quenched from 650° C)
OPTICAL DENSITY
.12
.1
.08
.06
.04
.02
536
537
538
539
540
WAVELENGTH (nm)

FIGURE 8

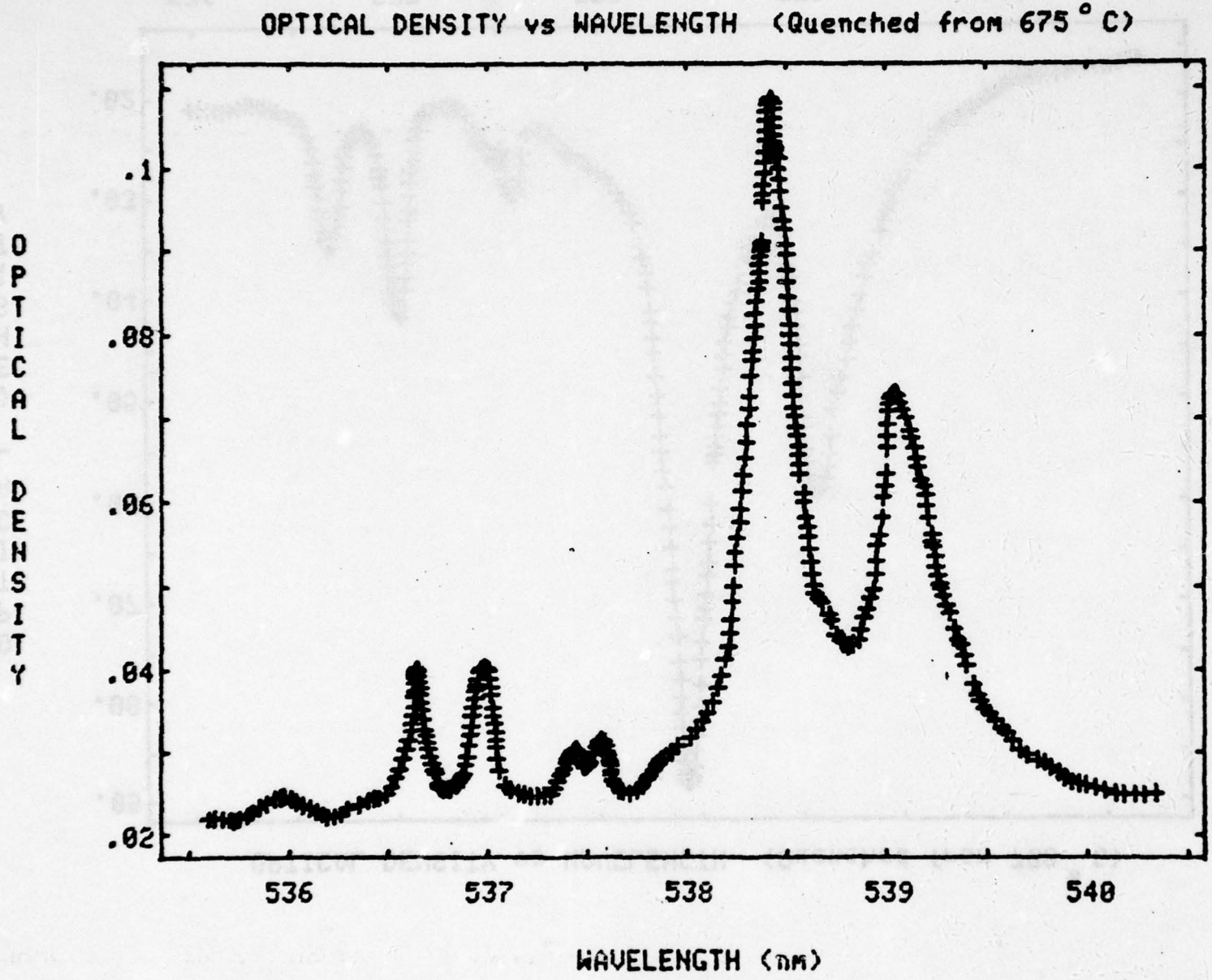
OPTICAL DENSITY vs WAVELENGTH (Quenched from 675 ° C)
OPTICAL DENSITY
.1
.08
.06
.04
.02
536
537
538
539
540
WAVELENGTH (nm)

FIGURE 9

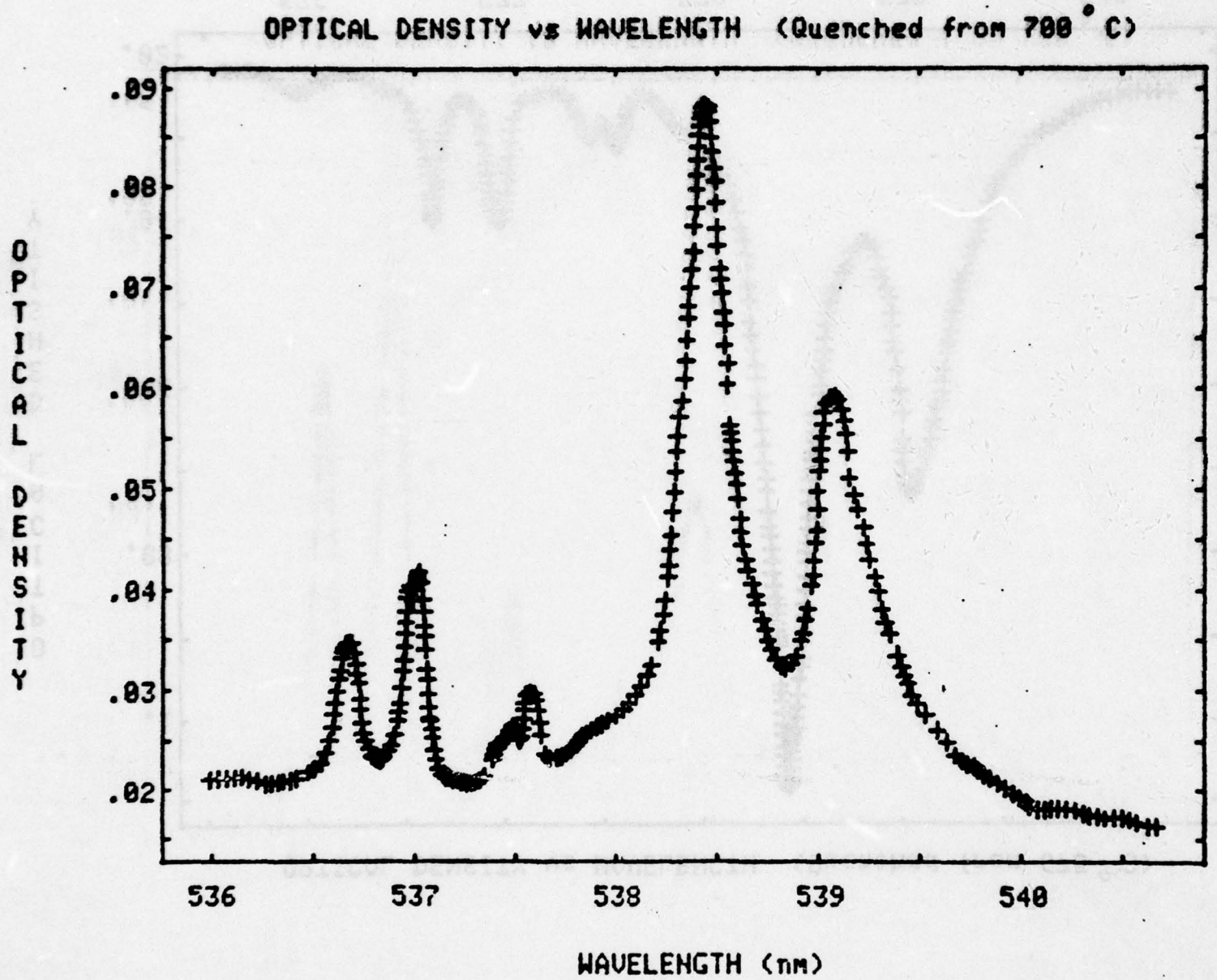
OPTICAL DENSITY vs WAVELENGTH (Quenched from 700 °C)
OPTICAL DENSITY
.09
.08
.07
.06
.05
.04
.03
.02
536
537
538
539
540
WAVELENGTH (nm)

FIGURE 10

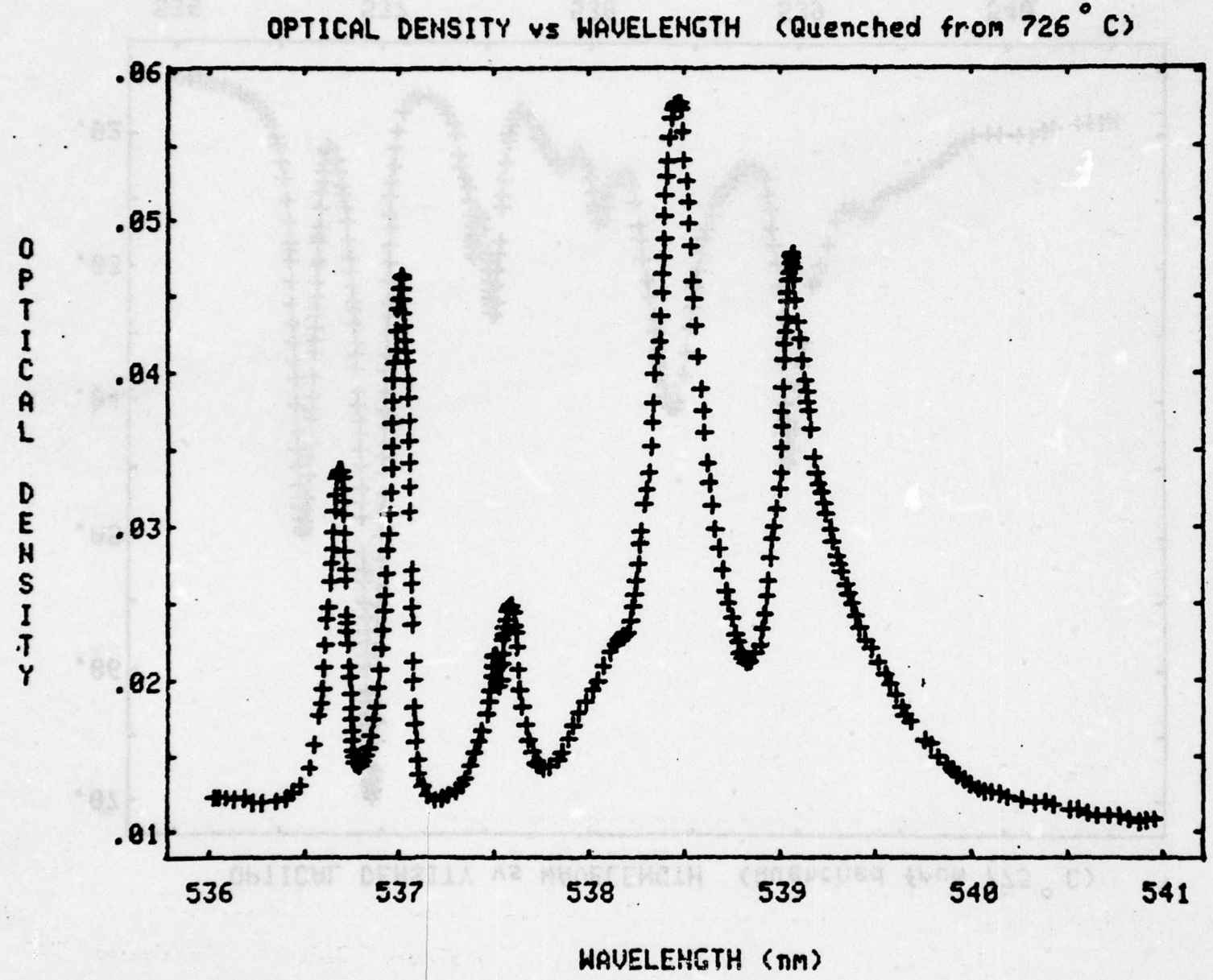
OPTICAL DENSITY vs WAVELENGTH (Quenched from 726 ° C)
OPTICAL DENSITY
.06
.05
.04
.03
.02
.01
536
537
538
539
540
541
WAVELENGTH (nm)

FIGURE 11

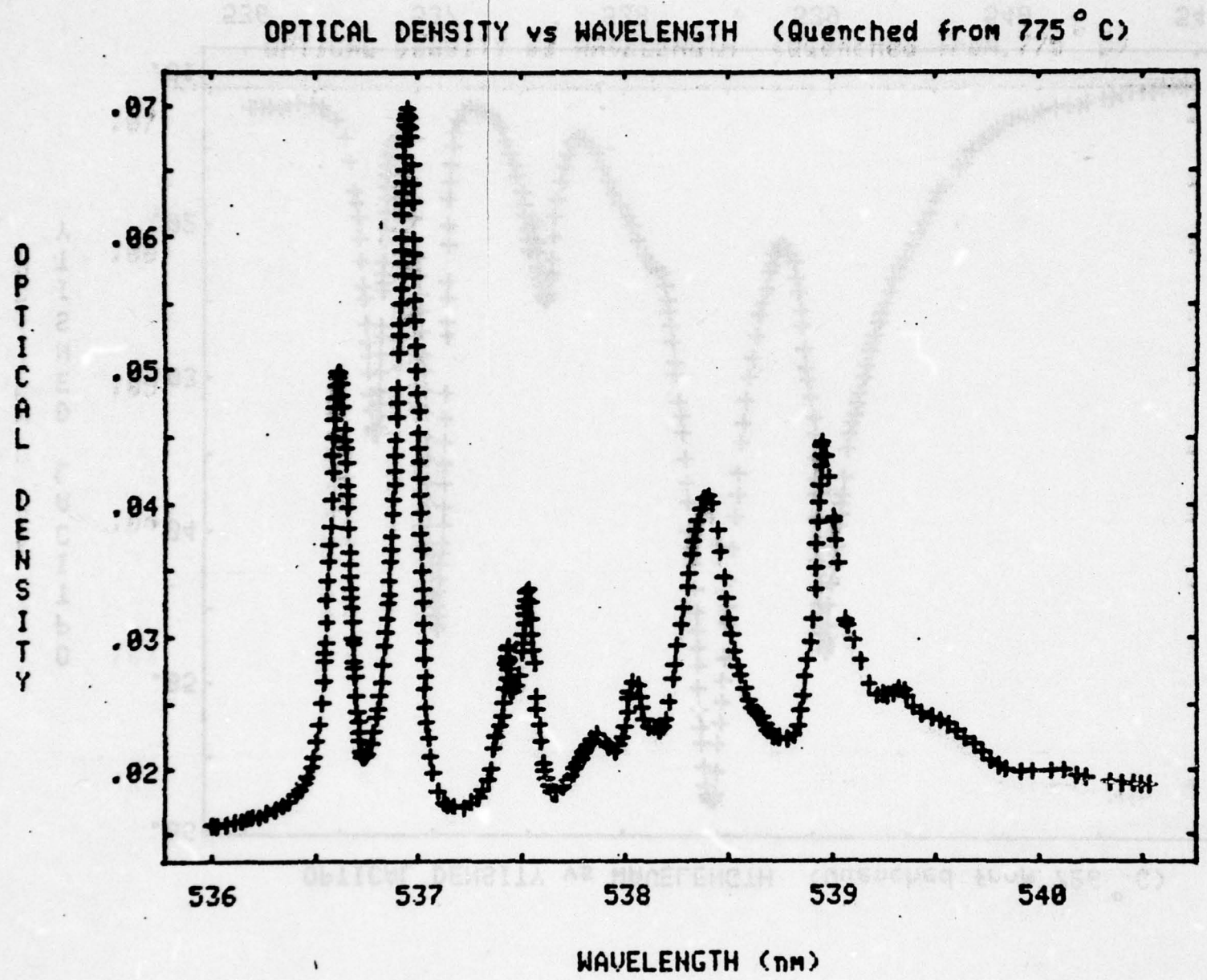
OPTICAL DENSITY vs WAVELENGTH (Quenched from 775° C)
OPTICAL DENSITY
.07
.06
.05
.04
.03
.02
536
537
538
539
540
WAVELENGTH (nm)

FIGURE 12

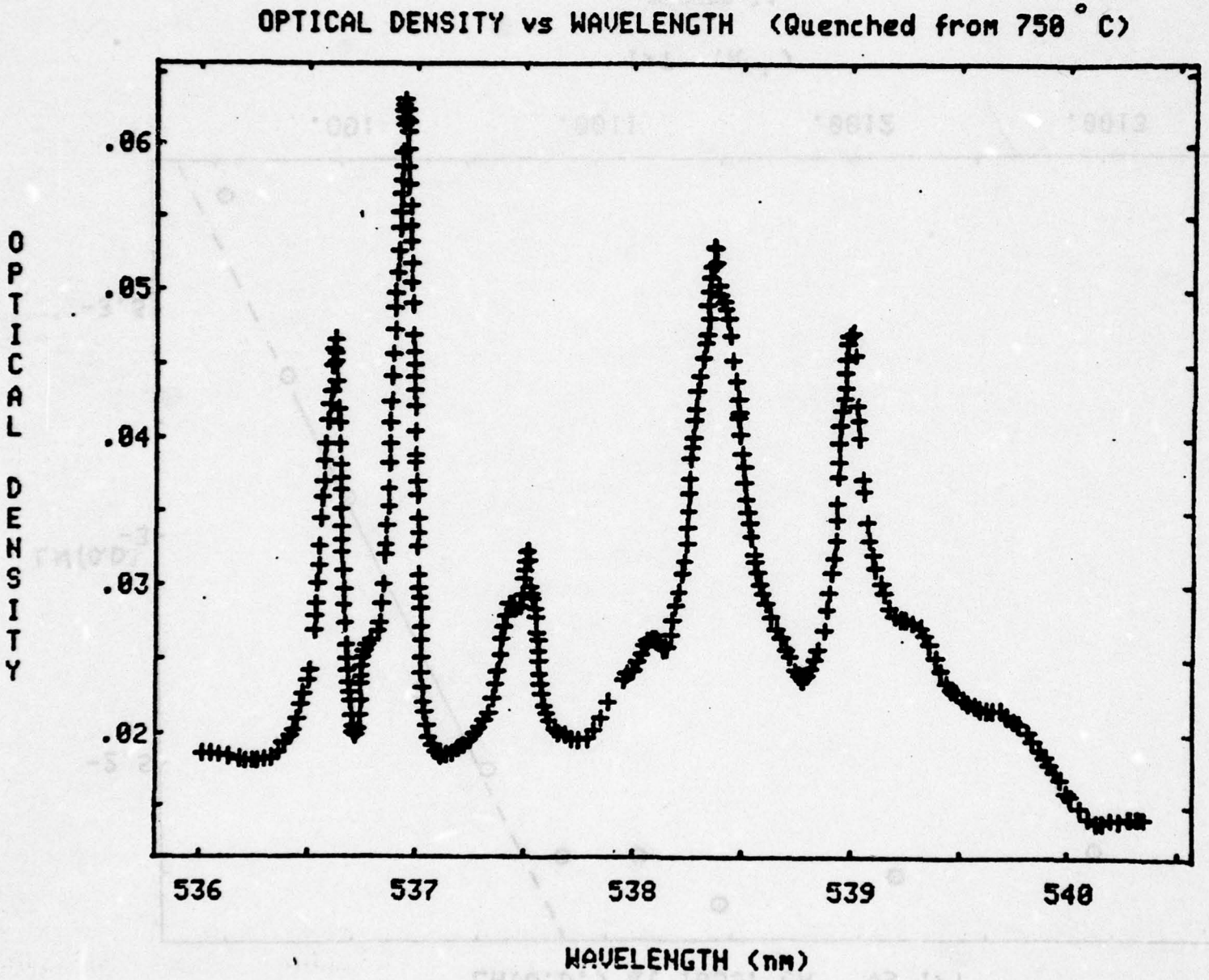
OPTICAL DENSITY vs WAVELENGTH (Quenched from 750 ° C)
OPTICAL DENSITY
.06
.05
.04
.03
.02
536
537
538
539
540
WAVELENGTH (nm)

FIGURE 13

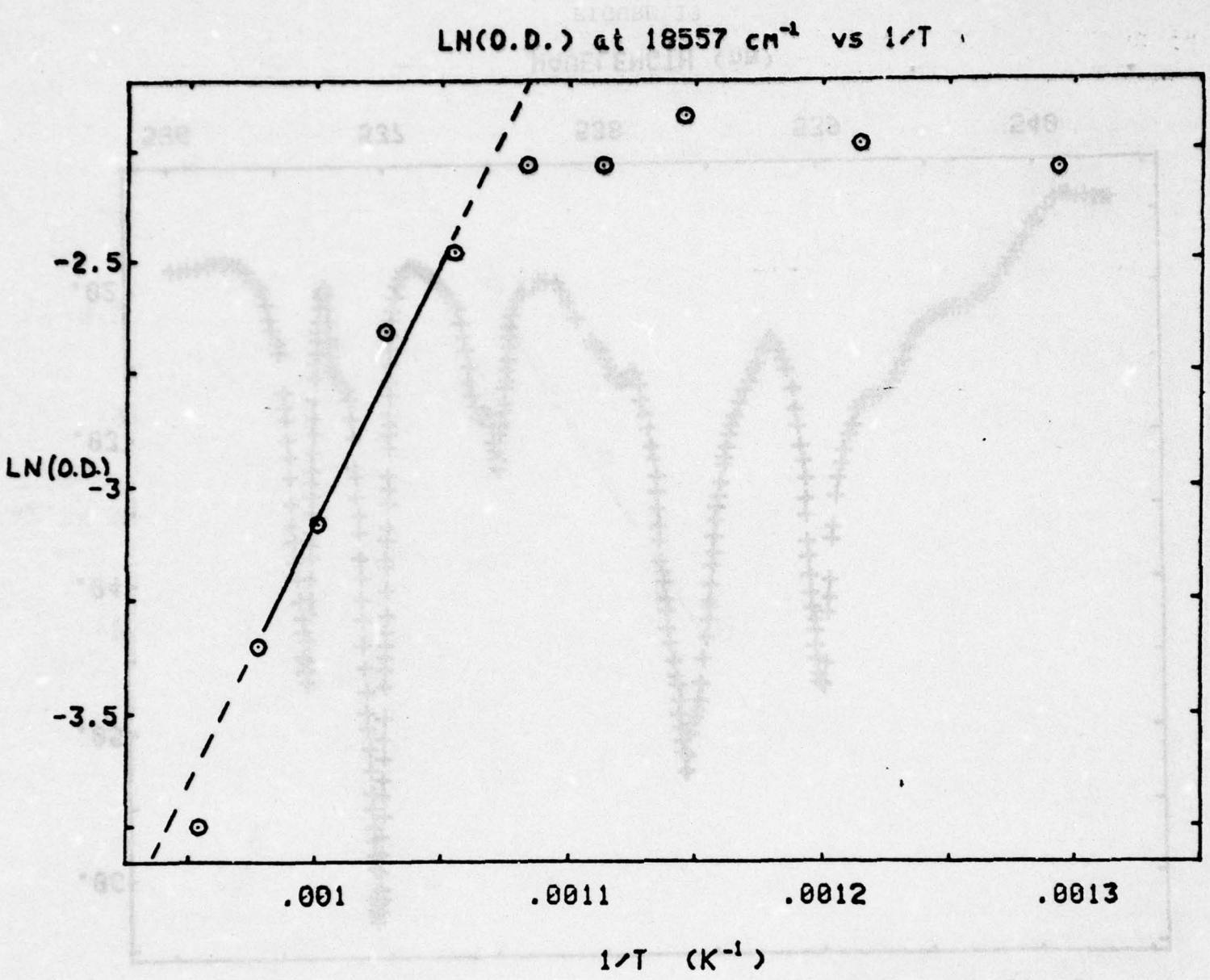

FIGURE 14

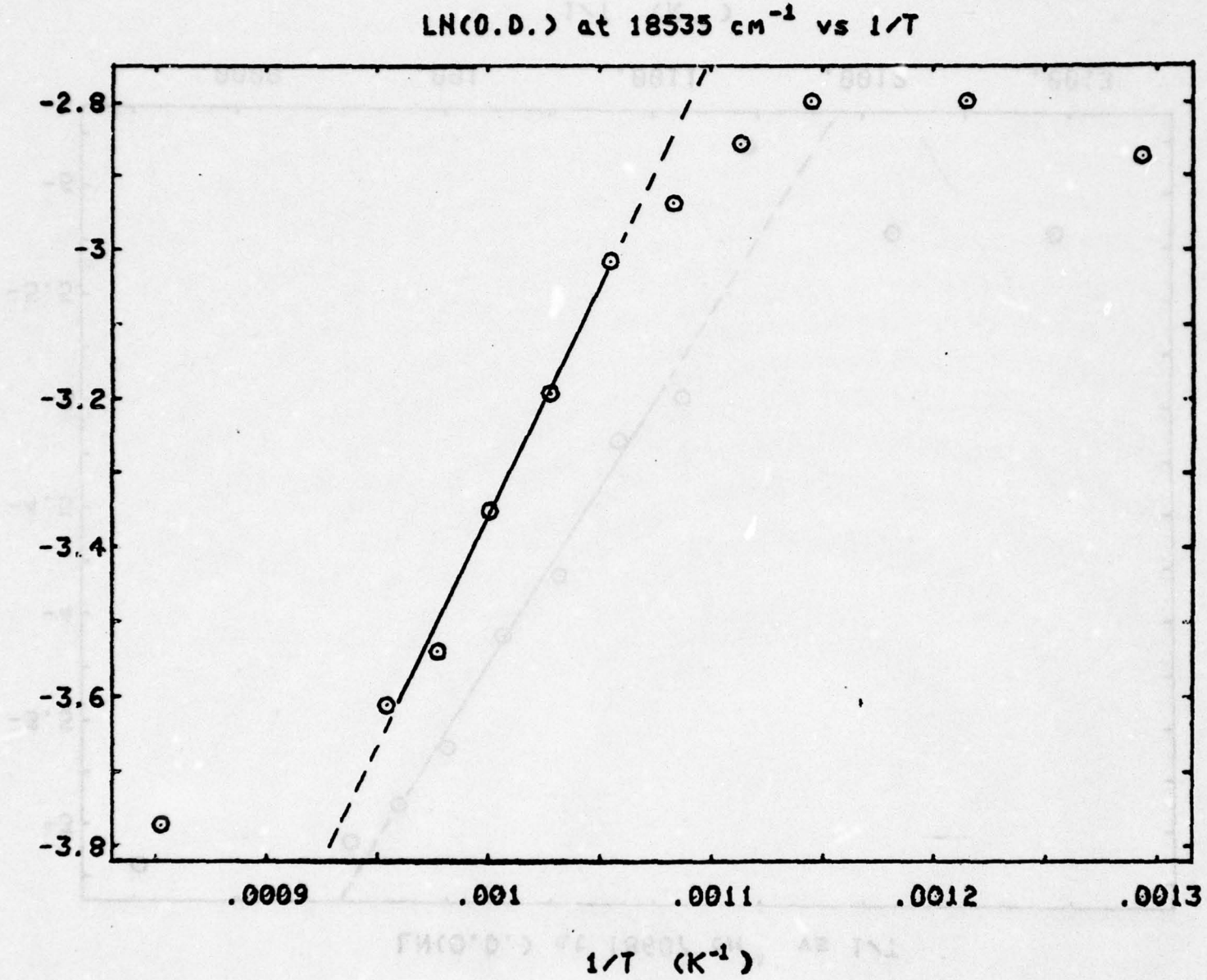
LN(O.D.) at 18535 cm^{-1} vs 1/T
LN(O.D.)
-2.8
-3
-3.2
-3.4
-3.6
-3.8
.0009
.001
.0011
.0012
.0013
1/T (K^{-1})

FIGURE 15

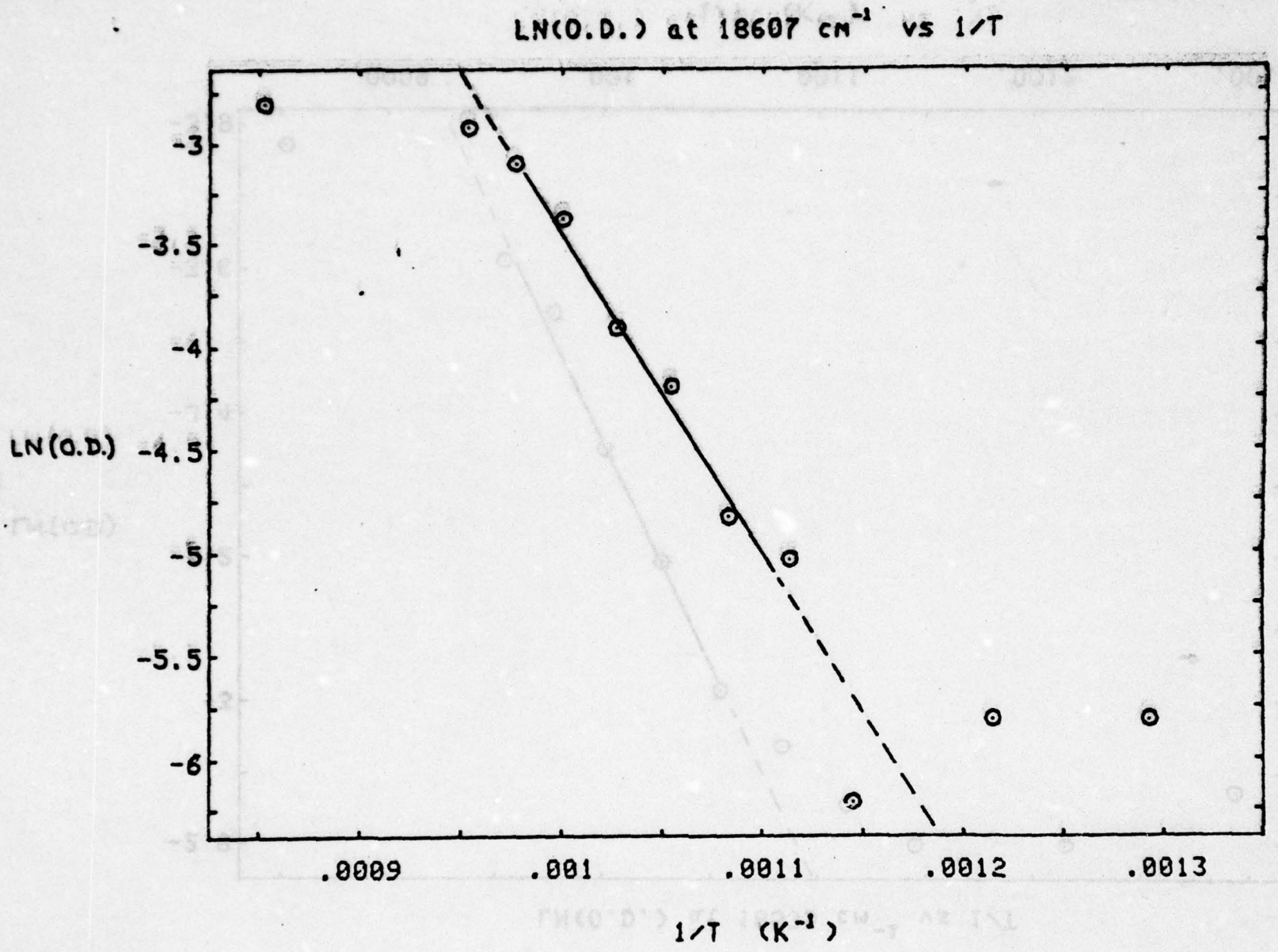
LN(O.D.) at 18607 cm^{-1} vs 1/T
LN(O.D.)
-3
-3.5
-4
-4.5
-5
-5.5
-6
.0009
.001
.0011
.0012
.0013
1/T (K^{-1})

FIGURE 16

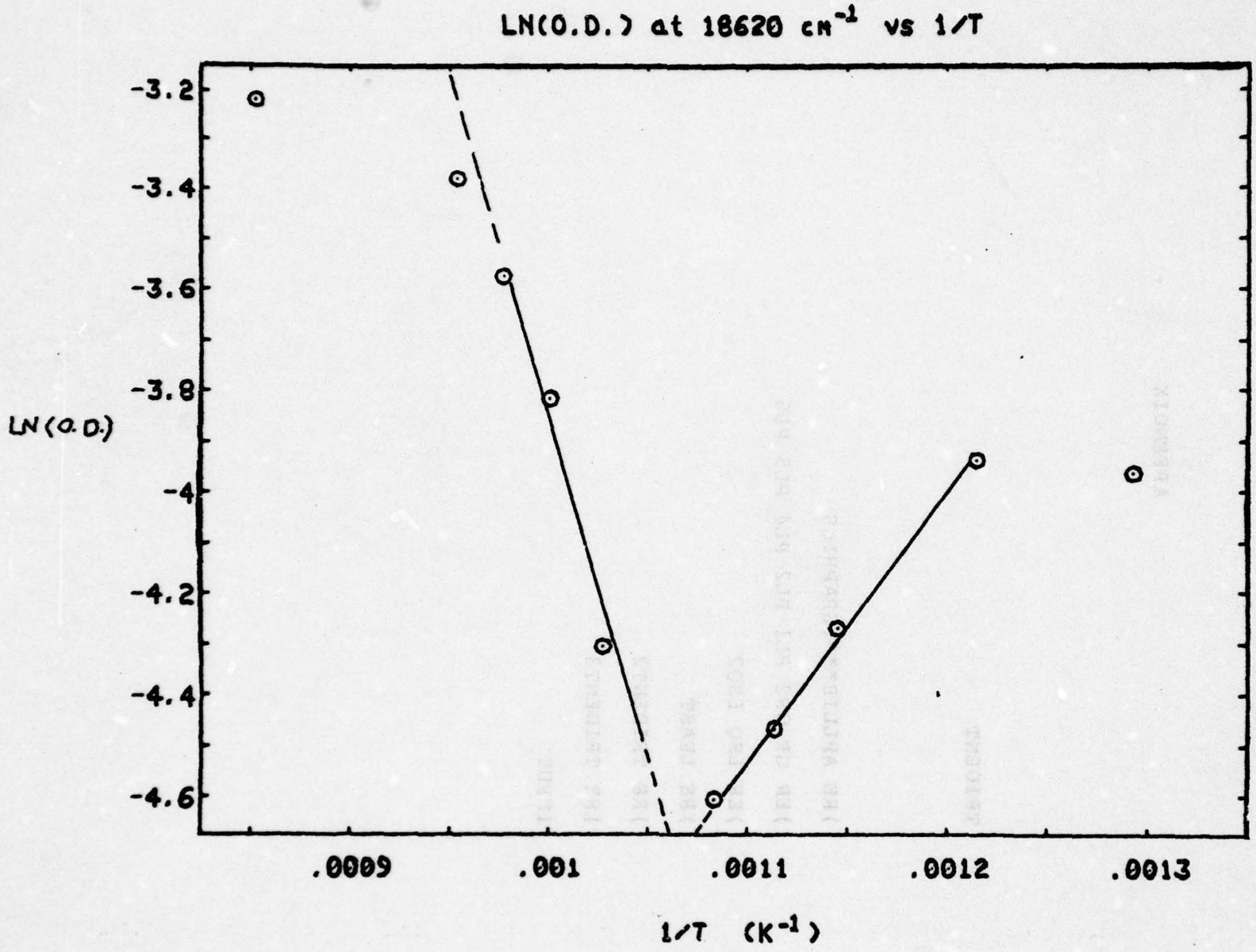
LN(O.D.) at 18620 cm^{-1} vs 1/T
-3.2
-3.4
-3.6
-3.8
-4
-4.2
-4.4
-4.6
LN(O.D.)
.0009
.001
.0011
.0012
.0013
1/T (K^{-1})

FIGURE 17

APPENDIX

```
TRIDENT


)RE APLLIB***:GRAPHICS
)ER GR GR2 PL1 PL2 PL4 PL5 PL6
)ER LSQ LSQ2
)RE LEAST
)RE TRIDENT2
)RE TRIDENT3
INPUT
```

```
LEAST

$     ZZ=FFN AA
[1]   .EPVVSET;
[2]   ZZ=.EPFF
$K
$     ZZ=DDER1 II;AA1;AA2
[1]   AA1=AA2=AA
[2]   AA1[II]=AA1[II]+DDA[II]
[3]   AA2[II]=AA2[II]-DDA[II]
[4]   ZZ=((FFN AA1)-FFN AA2)÷2#DDA[II]
$K
$     ZZ=II DDER2 JJ;AA1;AA2;AA3·AA4
[1]        CASE 1+II.NEJJ
[2]             DO
[3]             AA1=AA2=AA
[4]             AA1[II]=AA[II]+2#DDA[II]
[5]             AA2[JJ]=AA[JJ]-2#DDA[JJ]
[6]             ZZ=((FFN AA1)+FFN AA2)-2#FFN AA
[7]             END
[8]             DO
[9]             AA1=AA2=AA3=AA4=AA
[10]            AA1[II]=AA4[II]=AA[II]+DDA[II]
[11]            AA1[JJ]=AA3[JJ]=AA[JJ]+DDA[JJ]
```

```
[12]            AA2[II]=AA3[II]=AA[II]-DDA[II]
[13]            AA2[JJ]=AA4[JJ]=AA[JJ]-DDA[JJ]
[14]            ZZ=((FFN AA1)+FFN AA2)-(FFN AA3)+FFN AA4
[15]            END
[16]       END
[17] ZZ=ZZ%4#DDA[II]#DDA[JJ]
$K
$     WW1=WW;WW2;FF1;KK;LL
[1]   WW2=((.RO.EPXXNAME),0).ROKK=0
[2]       DO WHILE NN.GEKK=KK+1
[3]       WW2=WW2,DDER1 KK
[4]       END
[5]   KK=0;FF1=YY-FFN AA;WW1=(NN,NN).RO0;
[6]       DO WHILE NN.GEKK=KK+1
[7]       LL=KK-1
[8]            DO WHILE NN.GELL=LL+1
[9]            WW1[KK;LL]=WW1[LL;KK]=+/((KK DDER2
LL)#FF1)-WW2[;KK]#WW2[;LL]
[10]           END
[11]      END
$K
$     FF1=FFF;KK;FF2
[1]   FF1=.IO0;KK=0;FF2=YY-FFN AA;
[2]       DO WHILE NN.GEKK=KK+1
[3]       FF1=FF1,+/FF2#DDER1 KK
```

```
 [4]       END
 $K
 $     IITERATE
 [1]   AA=AA-FFF.IVWW
 $K
 $     SST=FIT
LLA;NNLIT;NN;AALIST;VVSET;KK;II;YY;XXNAME;FF;AA;DDA;NNI;SS;SS1;BB
 [1]   LLA=II.DALLA;FF=(II-
1)^LLA;II=LLA.IO';';NNLIT='123456789';
 [2]   LLA=II.DALLA;XXNAME=(II-1)^LLA;II=LLA.IO';';
 [3]   LLA=II.DALLA;AALIST=(II-1)^LLA;II=LLA.IO';';
 [4]   VVSET='';KK=0;NN=1++/',',.EQAALIST;
 [5]       DO WHILE NN.GEKK=KK+1
 [6]       II=AALIST.IO',
 [7]       VVSET=VVSET,(II-1)^AALIST
 [8]       AALIST=II.DAAALIST
 [9]       VVSET=VVSET,'=AA[',NNLIT[KK],'];'
 [10]      END
 [11] LLA=II.DALLA;NNI=.EP(II-1)^LLA;II=LLA.IO';';
 [12] LLA=II.DALLA;AA=,.EP(II-1)^LLA;II=LLA.IO';';
 [13] LLA=II.DALLA;DDA=,.EP(II-1)^LLA;II=LLA.IO';';
 [14] LLA=II.DALLA;.EPXXNAME,'=',(II-
1)^LLA;II=LLA.IO';';
 [15] YY=.EPLLA
 [16] KK=0;SS=+/(YY-FFN BB=AA)*2;
```

```
[17]      DO WHILE NNI.GEKK=KK+1
[18]      IITERATE
[19]      IF(SS%SS1=+/(YY-FFN AA)*2)<1
[20]      THEN KK=NNI;SST=0;AA=BB;
[21]      ELSE BB=AA;SS=SS1;SST=1;
[22]      END
[23] .EPVVSET;
[24] OOUT:@=(SS%.ROYY)*0.5;.QQ='RMS DEVIATION:';
[25] KK=0
[26]      DO WHILE NN.GEKK=KK+1
[27]      II=VVSET.IO'=';
[28]      @=AA[KK];.QQ=((II-1)^VVSET),' =';
[29]      II=VVSET.IO';'
[30]      VVSET=II.DAVVSET
[31]      END
```

```
TRIDENT2


$K

$     Y=F L
[1]   Y=(B0#H#H)%(H#H)+4#(W-10000000%L)*2
$K
$     Y=G L;L1;L2;C;A;B
[1]   B=10000000#H%2#C;A=10000000#W%C=(W,H%2)+.#(W,H%2);
[2]   L1=L+X;L2=L-X;
[3]   Y=(L1#G1 L1)+(L2#G1 L2)-(L+L)#G1 L
[4]   Y=(Y+(2#G2 L)-(G2 L1)+G2 L2)%X#X
[5]   Y=(B0#H#H%4#C)#Y
$K
$     G=G1 S
[1]   S=S-A
[2]   G=S+A#.LG(S#S)+B#B
[3]   G=G+(((A+B)#A-B)%B)#"3.LOS%B
$K
$     G=G2 S
[1]   S=S-A
[2]   G=(S#(3#A)+0.5#S)+(((3#A#A)-B#B)%2)#.LG(S#S)+B#B
[3]   G=G+((A#(A#A)-3#B#B)%B)#"3.LOS%B
$K
```

```
$     Y=GG L;W;H;B0;X
[1]   W=W1;H=H1;B0=B1;X=X1;
[2]   Y=G L
[3]   W=W2;H=H2;B0=B2;X=X2;
[4]   Y=Y+G L
$K
$     Y=GGG L;W;H;B0;X
[1]   Y=GG L
[2]   W=W3;H=H3;B0=B3;X=X3;
[3]   Y=Y+G L
$K
$     TIME
[1]   @=' SECONDS';.QQ=(.IB21)%60;.QQ='TIME USED SO
FAR:';
$K
```

TRIDENT3

```
$     INPUT;ST;IN
[1]   @=CL
[2]   INP:FILE=.QQ;.QQ='DATA FILENAME ---> ';
[3]   ST=FILE.OP1
[4]   IF 1.EQ.RO,ST
[5]   THEN.GOINP;@=FILE,' COULD NOT BE OPENED.';
[6]   MM=Ø  2.ROØ
[7]   READ:IN=.IN1
[8]   IF&/1.E+37.LEIN
[9]   THEN.GOCLOSE
[10]  IF 2.EQ.RO,IN
[11]  THEN.GOREAD;MM=MM,[1]IN;
[12]  @='YOU HAVE PROBLEMS IN THE FORMAT OF ',FILE;
[13]  @=')EXITING APL AT THIS TIME.'
[14]  )EX
[15]  CLOSE:CV=1 1 7 5
[16]  CV=CV,.FL/MM[;1]
[17]  CV=CV,Ø
[18]  CV=CV,.CE/MM[;1]
[19]  CV=CV,1.1#.CE/MM[;2]
[20]  CV=CV,1 1 1 1 3 Ø  Ø  1
[21]  OFF=.FL/MM[;2]
```

```
[22]       DO WHILE 0.NE.RO,IN=.IN1
[23]       W=IN[1];H=IN[2];B0=IN[3];X=IN[4];
[24]       MM[;2]=MM[;2]-G MM[;1]
[25]       END
[26] M=MM
[27] B0=.CE/MM[;2]
[28] H=1
[29] X=0.06
[30] W=1000000%0.5#(.CE/MM[;1])+.FL/MM[;1]
[31] MODE=1
$K
$     PL;Y
[1]   L=0,.IO100
[2]   L=CV[5]+(0.01#-/CV[7 5])#L
[3]   @=CL
[4]   CV DRAW M
[5]   CW=CV[.IO8],0  0  4 0  0  1 0  1
[6]       CASE MODE
[7]       CW DRAW L,Y=OFF+G L
[8]       CW DRAW L,Y=OFF+GG L
[9]       CW DRAW L,Y=OFF+GGG L
[10]      END
$K
$     NEW VARS;L;OD
[1]   L=M[;1]
```

```
 [2]  OD=M[;2]
 [3]        CASE MODE
 [4]        FIT 'OFF+G
L;L;',VARS,';1;',VARS,';0.5.FL0.05#',VARS,';L;OD'
 [5]        FIT 'OFF+GG
L;L;',VARS,';1;',VARS,';0.5.FL0.05#',VARS,';L;OD'
 [6]        FIT 'OFF+GGG
L;L;',VARS,';1;',VARS,';0.5.FL0.05#',VARS,';L;OD'
 [7]        END
 [8]  TIME
$K
$     RANGE;I
 [1]  CV=1 1 7 5
 [2]  CV=CV,.EP.QQ;.QQ='LEFT ---> ';
 [3]  CV=CV,0,.EP.QQ;.QQ='RIGHT ---> ';
 [4]  I=MM[;1].GECV[5]
 [5]  I=I&MM[;1].LECV[7]
 [6]  M=I/[1]MM
 [7]  CV=CV,1.1#.CE/M[;2]
 [8]  CV=CV,1 1 1 1 3 0  0  1
 [9]  B0=B1=B2=B3=.CE/M[;2]
 [10] H=H1=H2=H3=1
 [11] X=X1=X2=X3=0.06
 [12] W3=W=10000000%0.5#(.CE/M[;1])+.FL/M[;1]
 [13] W2=.5#W+10000000%.CE/M[;1]
```

```
[14] W1=.5#W+10000000%.FL/M[;1]
$K
$     SUBTRACT
[1]         CASE MODE
[2]              DO MM[;2]=MM[;2]-G MM[;1]
[3]              (W,H,B0,X).PR1
[4]              END
[5]              DO MM[;2]=MM[;2]-GG MM[;1]
[6]              (W1,H1,B1,X1).PR1
[7]              (W2,H2,B2,X2).PR1
[8]              END
[9]              DO MM[;2]=MM[;2]-GGG MM[;1]
[10]             (W1,H1,B1,X1).PR1
[11]             (W2,H2,B2,X2).PR1
[12]             (W3,H3,B3,X3).PR1
[13]             END
[14]        END
$K
$     R=RMS
[1]         CASE MODE
[2]         R=((+/R#R)%.ROR=M[;2]-OFF+G M[;1])*0.5
[3]         R=((+/R#R)%.ROR=M[;2]-OFF+GG M[;1])*0.5
[4]         R=((+/R#R)%.ROR=M[;2]-OFF+GGG M[;1])*0.5
[5]         END
$K
```

CURVE

```
)RE *G05037:TRIDENT2
$     THEORY
[1]   OFF=.EP.QQ;.QQ='OFFSET ---> ';
[2]   INP:FILE=.QQ;.QQ='DATA FILENAME ---> ';
[3]   ST=FILE.OP1;NP="1;
[4]   IF 0.NE.RO,ST THEN.GOINP
[5]   RESET
[6]   .GO(0.NE.RO,.IN1)/.IB26;NP=NP+1;
[7]   RESET
[8]   L=.EP.QQ;.QQ='LEFT ---> ';
[9]   L=L+((R=.EP.QQ)-L)#(0,.IO100)&100;.QQ='RIGHT --->
';
[10]  N=0;YF=YG=OFF;
[11]        DO WHILE NP.GEN=N+1
[12]        W=IN[1];H=IN[2];IN=.IN1;
[13]        L=L,(("".08#H)+1.E+7&W)+.004#H#0,.IO40
[14]        END
[15]  RESET;L=L[.GUL];N=0;
[16]        DO WHILE NP.GEN=N+1
[17]        IN=.IN1
[18]        W=IN[1];H=IN[2];B0=IN[3];X=IN[4];
[19]        YF=YF+F L
```

```
 [20]       YG=YG+G L
 [21]       END
 [22] .CL1
 [23] FILE:F=.QQ;.QQ='FILE INTO WHICH CURVE POINTS ARE
TO BE WRITTEN ---> ';
 [24] ST=F.OP1
 [25] IF 0.NE.RO,ST THEN.GOFILE;@=F,' COULD NOT BE
OPENED.';
 [26] N=0
 [27]       DO WHILE (.ROL).GEN=N+1
 [28]       (L[N],YG[N]).PR1;
 [29]       END
 [30] N=0;'1E37 1E37'.PR1;
 [31]       DO WHILE (.ROL).GEN=N+1
 [32]       (L[N],YF[N]).PR1;
 [33]       END
 [34] .CL1;'1E37 1E37'.PR1;
 $K
 $     R=RESET
 [1]   R=.IO0;.ST1;
 [2]   .GO(.OR/1E37.GT.IN1)/.IB26
 $K
 THEORY
```

UNCLASSIFIED

SECURITY CLASSIFICATION OF THIS PAGE (When Data Entered)

REPORT DOCUMENTATION PAGE		READ INSTRUCTIONS BEFORE COMPLETING FORM
1. REPORT NUMBER U.S.N.A. - TSPR; no. 97 (1979)	2. GOVT ACCESSION NO.	3. RECIPIENT'S CATALOG NUMBER
4. TITLE (and Subtitle) THE KINETICS OF ION MOTION IN CaF_2 : ER.		5. TYPE OF REPORT & PERIOD COVERED Final: 1978, 1979. 6. PERFORMING ORG. REPORT NUMBER
7. AUTHOR(s) David Alan Beam.		8. CONTRACT OR GRANT NUMBER(s)
9. PERFORMING ORGANIZATION NAME AND ADDRESS United States Naval Academy, Annapolis.		10. PROGRAM ELEMENT, PROJECT, TASK AREA & WORK UNIT NUMBERS
11. CONTROLLING OFFICE NAME AND ADDRESS United States Naval Academy, Annapolis		12. REPORT DATE 8 June 1979. 13. NUMBER OF PAGES 59
14. MONITORING AGENCY NAME & ADDRESS(if different from Controlling Office)		15. SECURITY CLASS. (of this report) UNCLASSIFIED 15a. DECLASSIFICATION/DOWNGRADING SCHEDULE

16. DISTRIBUTION STATEMENT (of this Report)

This document has been approved for public release;
its distribution is UNLIMITED.

17. DISTRIBUTION STATEMENT (of the abstract entered in Block 20, if different from Report)

This document has been approved for public release;
its distribution is UNLIMITED.

18. SUPPLEMENTARY NOTES

Accepted by the U.S. Trident Scholar Committee.

19. KEY WORDS (Continue on reverse side if necessary and identify by block number)

Calcium fluorides -- Defects.
Erbium -- Defects.
Ion flow dynamics.
Ionic equilibrium.

20. ABSTRACT (Continue on reverse side if necessary and identify by block number)

The kinetics of ion motion in rare-earth doped calcium fluoride crystals (CaF_2: ER 3+) was optically observed as they were subjected to various heating and annealing sequences. This annealing studies was made at temperatures ranging from 300 C to 900 C. Optical studies was covered the spectral range from 250 nm to 600 nm. The sample was kept at about 10K while the optical spectra has been recorded. The variation in concentration of defects as a function of annealing temperature was measured. This yields information about

OVER !

DD FORM 1 JAN 73 1473 EDITION OF 1 NOV 65 IS OBSOLETE
S/N 0102-014-6601 |

UNCLASSIFIED.

SECURITY CLASSIFICATION OF THIS PAGE (When Data Entered)

CONTINUED:

the equilibrium existing among the different defect configurations as a function of temperature. - The resultant temperature dependence was analyzed to determine the energy of motion for the ion responsible for maintaining the equilibrium. -

0 - 0